

**Supplementary Information for  
Calibrating the co-evolution of Ediacaran life and environment**

Alan D. Rooney, Marjorie D. Cantine, Kristin D. Bergmann, Thomas H. Boag, James F. Busch,  
Erik A. Sperling, Justin V. Strauss

Alan D. Rooney and Marjori D. Cantine.  
E-mail: [alan.rooney@yale.edu](mailto:alan.rooney@yale.edu) [mcantine@mit.edu](mailto:mcantine@mit.edu)

This PDF file includes:  
Supplementary text  
Figs. S1 to S3  
Tables S1 to S3  
Supplementary File references

## **Supplementary Information Text**

### Geological Setting: Oman

The Ediacaran Nafun Group of Oman is exposed in outcrop in the southern Huqf Desert and northern Oman Mountains (Al Hajar Mountains) and is extensively penetrated by drillcore in the South Oman Salt Basin and Huqf-Haushi High areas (Fig. S1). In the subsurface and Huqf Desert, the Nafun Group is exceptionally well-preserved and has not undergone significant metamorphism or burial. The sedimentology, stratigraphy, and geochemistry of the Nafun Group has been extensively studied (1-23), in part motivated by the presence of hydrocarbon resources and in part because its exceptional preservation offers the opportunity to study proxy records that have been obscured or obliterated in many other Ediacaran successions. Proxy records examined in Oman have included carbonate clumped isotopes (15), biomarkers (5-7, 12) and carbonate-associated sulphate (10, 11).

The Nafun Group overlies the Abu Mahara Group, which contains diamictites correlated with Cryogenian glaciations, and the Nafun Group's basal Hadash Formation (Fm) is correlated with the post-Marinoan cap carbonate globally. The Nafun Group is a mixed siliciclastic-carbonate deposit with two major cycles of siliciclastic-to-carbonate deposition. The lower cycle is represented by the Masirah Bay and Khufai formations, and the upper cycle by the Shuram and Buah formations. Both cycles are characterized by lithofacies assemblages consistent with a shallowing upwards pattern (15).

The Masirah Bay overlies the Hadash Fm, the Cryogenian Ghadir Manquil Fm, or the Halfayn volcanic suite depending on the location. The Masirah Bay Fm is dominantly siliciclastic, with shales, siltstones, and sandstones, though it contains interbedded shales and dolomites near its top (16). Its upper contact with the Khufai Fm is transitional, from thinly bedded shales and dolomites into continuous carbonate (21). The Khufai Fm contains both limestones and dolomites and was deposited in a ramp setting (11, 21). Fetid carbonates are common, as are grainstones and silicification. The onset of the Shuram CIE is captured in the uppermost Khufai Fm, and its contact with the Shuram Fm in the Huqf Desert is marked by a laterally continuous oolite on which cauliform stromatolites nucleated (2; Table S1). The transition to the Shuram Fm is also marked by a sharp shift to siliciclastic siltstone with occasional interbedded limestones, which increase in abundance moving upsection (2, 9, 21). Shuram Fm limestones often contain ooids and edgewise conglomerates and siltstones in the Huqf Desert typically contain hummocky and swaley cross

stratification (9, 21). Full recovery to positive  $\delta_{13}\text{C}$  values occurs in the overlying, carbonate-dominated Buah Fm (2, 3, 19, 21, 23; Fig. S2; Table S1). In deep-water sections, a thick silicilite (rock containing >90% cryptocrystalline silica) occurs in the upper Buah Fm. An unconformity between the Buah Fm and the overlying carbonates and evaporites of the Ara Group is often seen in the subsurface, while in the Oman Mountains, the Buah is overlain by the volcaniclastics of the Fara Fm (16).

Radioisotopic constraints on the Nafun Group are limited to minimum depositional ages derived from detrital zircons (17). Extensive dating of volcaniclastic and ash units in the overlying Ara Group from the Oman Mountains and South Oman Salt Basin have yielded latest Ediacaran ages (17). Fossils of Ediacaran biota are not known from any Nafun Group stratigraphy, but Cloudina and Namacalathus are reported in Ara Group drillcore (20).

Two drillcores, drilled by Petroleum Development Oman in the last decade, sample the deepest water environments of the South Oman Salt Basin (Fig. S1). We refer to them as Well L and Well M. Carbon isotope data, sedimentology, and gamma ray data guide the correlation of these cores both to other subsurface wells and to outcrop in the Huqf Desert and Oman Mountains. Correlation of Wells L and M to Thamoud-6, a well that has been previously described is shown in Figs. S1, S2), with stratigraphic location of Re-Os samples sampled for this study. Organic-rich shale intervals were targeted for Re-Os geochronology. Sample suites comprise up to 9 subsamples taken within intervals up to 1.4 meters in total thickness.

#### Geological Setting: NW Canada

In the Wernecke and Ogilvie Mountains of Yukon, Canada, Neoproterozoic rocks of the Windermere Supergroup (ca. 780-540 Ma) consist of a ca. 6 km thick mixed carbonate-siliciclastic succession deposited along the northwestern margin of Laurentia (24-26). Ediacaran strata of the Wernecke Mountains comprise the recently formalized Rackla Group (27), which is composed of the Sheepbed, Nadaleen, Gametrail, Blueflower, Algae, and Risky formations (24, 25, 27-30; Fig. S3). The ca. 632 Ma Sheepbed Formation locally overlies glaciogenic diamictite (Rapitan Group) and cap carbonate (Ravensthorpe Formation) of the Cryogenian Marinoan glaciation (27, 28, 31-34). These strata are overlain by mixed siliciclastic and carbonate strata of the Nadaleen Formation, which locally contains the Ediacaran macrofossil Aspidella and are characterized by highly enriched  $\delta_{13}\text{C}_{\text{carb}}$  values up to +9‰ (ref. 27). The overlying Gametrail

Formation contains highly depleted  $\delta_{13}\text{C}_{\text{carb}}$  values down to -13‰ that have been correlated globally with the Shuram CIE (27, 28; Table S1); this unit records an abrupt return to positive  $\delta_{13}\text{C}_{\text{carb}}$  values near the top of the formation and its contact with the overlying Blueflower Formation (Fig. 1; Extended Data Fig. 3). The Gametrail Formation is overlain by mixed siliciclastic and carbonate strata of the fossiliferous Blueflower, Algae, and Risky formations, the latter of which lies at or just below the Ediacaran-Cambrian boundary (25, 29, 35-37).

Ediacaran–Cambrian strata of the Ogilvie Mountains comprise a series of informal map units labeled PH3, PH4, and PH5 (28, 38-41; Fig. S3). Units PH3 and PH4 were previously correlated with the informal “upper group” (28), but recent formalization of the Rackla Group suggests these units instead belong within this newer lithostratigraphic unit (27). Unit PH3 consists predominantly of black shale and mudstone that directly overlies an unnamed Cryogenian glacial deposit and cap carbonate pair belonging to the ca. 635 Ma Marinoan glaciation (28, 39). This is succeeded by unit PH4, which is composed primarily of hummocky cross-stratified dolostone, silty dolostone, and rare dolorudstone with interbedded black shale and concretionary limestone near its top. These strata record highly depleted  $\delta_{13}\text{C}_{\text{carb}}$  values down to -9‰, which have previously been correlated with the Shuram CIE (27; Table S1). The concretionary limestone unit at the top of unit PH4 has been loosely correlated with the Blueflower Formation and records a return to enriched  $\delta_{13}\text{C}_{\text{carb}}$  values (Fig. S3). Locally, units PH3 and PH4 are truncated by an angular unconformity beneath unit PH5, which is composed of siltstone and sandstone that contain diagnostic early-middle Cambrian trace fossils including *Skolithos*, *Cruziana*, and *Rusophycus* (38).

### Re-Os geochronology

All radioisotopic analyses were performed at the Yale University Metal Geochemistry and Geochronology Center. Weathered surfaces were removed with a diamond-encrusted rock saw and samples were then hand-polished using a diamond-encrusted polishing pad to remove cutting marks and eliminate any potential for contamination from the saw blade. The samples were dried overnight at ~40 °C and then crushed to a fine (~30 µm) powder in a SPEX 8500 Shatterbox using a zirconium ceramic grinding container and puck in order to homogenize any Re and Os heterogeneity present in the samples (42). The Re and Os isotopic abundances and compositions were determined following methodologies previously described (43, 44).

Between 0.15 and 1 g of sample was digested and equilibrated in 8 ml of Cr<sub>vI</sub>O<sub>3</sub>-H<sub>2</sub>SO<sub>4</sub> together with a mixed tracer (spike) solution of <sup>190</sup>Os and <sup>185</sup>Re in carius tubes at 220 °C for 48 hours. Rhenium and Os were isolated and purified using solvent extraction (NaOH, (CH<sub>3</sub>)<sub>2</sub>CO, and CHCl<sub>3</sub>), micro-distillation and anion column chromatography methods, as outlined previously (45, 46). The Cr<sub>vI</sub>O<sub>3</sub>-H<sub>2</sub>SO<sub>4</sub> digestion method was employed as it has been shown to preferentially liberate hydrogenous Re and Os yielding more accurate and precise age determinations (47, 48). Total procedural blanks during this study were  $88.0 \pm 2.1$  pg and  $0.18 \pm 0.07$  pg for Re and Os respectively, with an average <sup>187</sup>Os/<sup>188</sup>Os value of  $0.25 \pm 0.05$  ( $1\sigma$ ,  $n = 4$ ). The major source (>90%) of Re blank is from the Cr<sub>vI</sub>O<sub>3</sub>-H<sub>2</sub>SO<sub>4</sub> solution.

Isotopic measurements were performed using a ThermoFisher TRITON PLUS thermal ionization mass spectrometer in negative mode at the Yale University via static Faraday collection for Re and ion-counting using a secondary electron multiplier in peak-hopping mode for Os (49, 50). The Os samples were loaded onto 99.995% Pt wire (H-Cross, NJ) in 9 N HBr and covered with a saturated solution of Ba(OH)<sub>2</sub> in 0.1 N NaOH as activator and analyzed as oxides of Os. Interference of <sup>187</sup>ReO<sub>3</sub> on <sup>187</sup>OsO<sub>3</sub> was corrected by the measured intensity of <sup>185</sup>ReO<sub>3</sub>. Mass fractionation was corrected with <sup>192</sup>Os/<sup>188</sup>Os = 3.0826, using the exponential fractional law. Measurement quality was monitored by repeated measurement of the DROsS standard solution, which yielded <sup>187</sup>Os/<sup>188</sup>Os values of  $0.16091 \pm 0.00015$  ( $n=51$ ) over the course of the measurement campaign, in good agreement with values obtained by other laboratories (51, 52). The Yale University Re standard solution (measured on faraday cups during analytical sessions) yields an average <sup>185</sup>Re/<sup>187</sup>Re value of  $0.59783 \pm 0.0006$ ; ( $1\sigma$ ,  $n = 17$ ), which is indistinguishable, within uncertainty previously published values (53). The measured difference in <sup>185</sup>Re/<sup>187</sup>Re values for the Re solution and the accepted <sup>185</sup>Re/<sup>187</sup>Re value of 0.59738; previously published values (53) are used to correct the Re sample data for instrument mass fractionation and blank and spike contributions.

Uncertainties for <sup>187</sup>Re/<sup>188</sup>Os and <sup>187</sup>Os/<sup>188</sup>Os are determined by error propagation of uncertainties in Re and Os mass spectrometry measurements, blank abundances and isotopic compositions, spike calibrations, and reproducibility of standard Re and Os isotopic values. The Re-Os isotopic data,  $2\sigma$  calculated uncertainties for <sup>187</sup>Re/<sup>188</sup>Os and <sup>187</sup>Os/<sup>188</sup>Os, and the associated error correlation function (rho) are regressed to yield a Re-Os date using Isoplot V. 4.15 with the  $\lambda_{187}\text{Re}$  constant of  $1.666 \times 10^{-11}\text{a}^{-1}$  (54-56). Elemental concentrations and isotopic compositions

for the Re-Os geochronology samples are listed in Table S2. All samples display enrichments above average crustal values with Re abundances ranging from 0.64 to 245.1 ng/g and Os abundances from 56 to 4703 pg/g.

#### Carbon and Oxygen Isotope Geochemistry

Carbonate rock samples from northwestern Canada were analyzed at both Dartmouth College and the Yale Analytical and Stable Isotope Center. 0.1-0.5 kg samples of limestone and dolostone were collected approximately every m throughout detailed measured stratigraphic sections and targeted to avoid obvious fracturing or veining. The samples were then slabbed perpendicular to bedding using a lapidary saw and ~ 5-10 mg of powder was drilled from individual laminations using a drill press with a dental carbide drill bit. Carbonate powders analyzed at Dartmouth College (JB1704, J1711, JB1707, T1701, J1713, JB1801) were reacted with phosphoric acid ( $H_3PO_4$ ) at 70°C on a Gasbench II preparation device attached to a ThermoFinnigan DeltaPlus XL continuous flow isotope ratio mass spectrometer.  $\delta^{13}C_{carb}$  and  $\delta^{18}O_{carb}$  were measured simultaneously and isotopic data are reported in standard delta notation as the per mil difference from VPDB (Vienna Pee Dee Belemnite). Precision and accuracy were monitored by running a total of 12 standards for every 76 samples using 11:3 sample/standard bracketing. The standard set includes two external standards (NBS-18 and Elemental Microanalysis (EM) Carrara Marble), as well as an internal marble standard. Samples are measured relative to an internal CO<sub>2</sub> gas standard and then converted to the VPDB scale using the known composition of NBS-18 ( $\delta^{13}C = -5.01$ ;  $\delta^{18}O = -23.20$ ) and the EM-Carrara Marble ( $\delta^{13}C_{carb} = 2.10$ ;  $\delta^{18}O_{carb} = -2.01$ ). Measured precision was 0.1-0.15‰ (1 $\sigma$ ) for  $\delta^{13}C_{carb}$  and 0.15-0.2‰ (1 $\sigma$ ) for  $\delta^{18}O_{carb}$ . Samples run at the Yale Analytical and Stable Isotopic Center (J1719) followed an identical procedure using a KIEL carbonate preparation device connected to a ThermoFinnigan MAT 253. The standard set includes the MERC ( $\delta^{13}C = -48.96$ ;  $\delta^{18}O = -16.48$ ), PX ( $\delta^{13}C_{carb} = 2.25$ ;  $\delta^{18}O_{carb} = -1.79$ ), and YM ( $\delta^{13}C_{carb} = -1.59$ ;  $\delta^{18}O_{carb} = -6.03$ ) standards which were calibrated against the NIBS 19, NBS 18, and LSVEC international standards on the VPDB scale. Internal precision was reported as 0.1-0.15‰ (1 $\sigma$ ) for  $\delta^{13}C_{carb}$  and 0.1-0.15‰ (1 $\sigma$ ) for  $\delta^{18}O_{carb}$ .

**Fig. S1:** Geological map of Oman, modified after published work (15, 16). Approximate locations of Wells L and M shown. Stratigraphic and chemostratigraphic overview of Wells L and M, with sampled horizons indicated.

**Fig. S2:** Lithostratigraphic and chemostratigraphic data for well Thamoud-6 with stratigraphic positions of samples from Well L and Well M shown. Formation boundaries follow Petroleum Development Oman's 2019 revision of stratigraphy. Recovery from the Shuram Excursion occurs within the Buah Fm.

**Fig. S3:** Geological map and detailed measured sections from Ediacaran strata in the Ogilvie and Wernecke Mountains, Yukon, Canada. The inset map shows the location of the measured sections in the main figure where NWT–Northwest Territories. Measured sections display main lithofacies and carbon isotope chemostratigraphy of the Rackla Group modified following published work (27, 28). The starred locations display the stratigraphic position of the sampled horizons.

**Table S1:**  $\delta_{13}\text{C}_{\text{carb}}$  isotope data were compiled from the literature from globally distributed successions (57-61). Published geochronological constraints and  $\delta_{13}\text{C}_{\text{carb}}$  chemostratigraphy were used to develop an age model.

**Table S2:** Rhenium and Os elemental abundance and isotopic composition data for isochron regressions. Uncertainties are given as  $2\sigma$  for  $^{187}\text{Re}/^{188}\text{Os}$  and  $^{187}\text{Os}/^{188}\text{Os}$  and  $^{192}\text{Os}$ . The uncertainty includes the  $2\sigma$  uncertainty for mass spectrometer analysis plus uncertainties for Os blank abundance and isotopic composition. (a) Rho is the associated error correlation (55). (b)  $\text{Osi}$  = initial  $^{187}\text{Os}/^{188}\text{Os}$  isotope ratio calculated at 578, 567, 575, 562 and 574 Ma.

**Table S3:** In addition to ages from this work, some ages used for the construction of Figure 3 are from previously published work (17, 31, 62-66). Ages published before 2012 are as recalculated (67); ages are color-coded to their region of origin. All uncertainties include relevant decay constant uncertainties. The \* indicates U-Pb zircon chemical abrasion isotope dilution thermal ionization mass spectrometry (CA-ID-TIMS) age; † indicates U-Pb zircon Sensitive High-

Resolution Ion Microprobe (SHRIMP) age; ‡indicates Re-Os organic-rich rock age. Ages from this study are bolded.

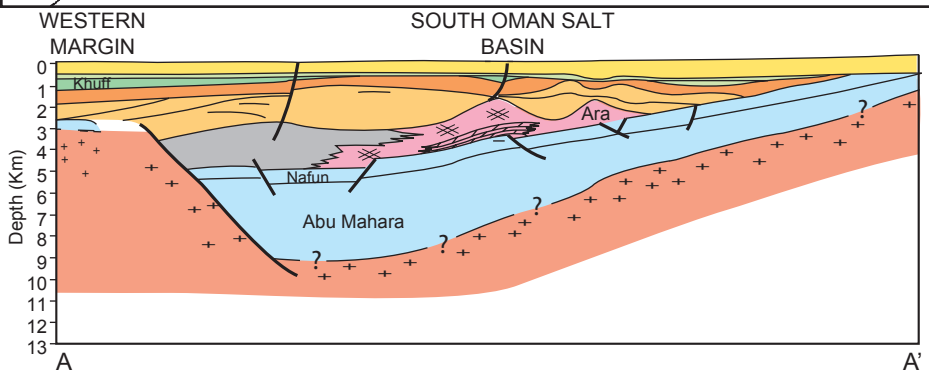
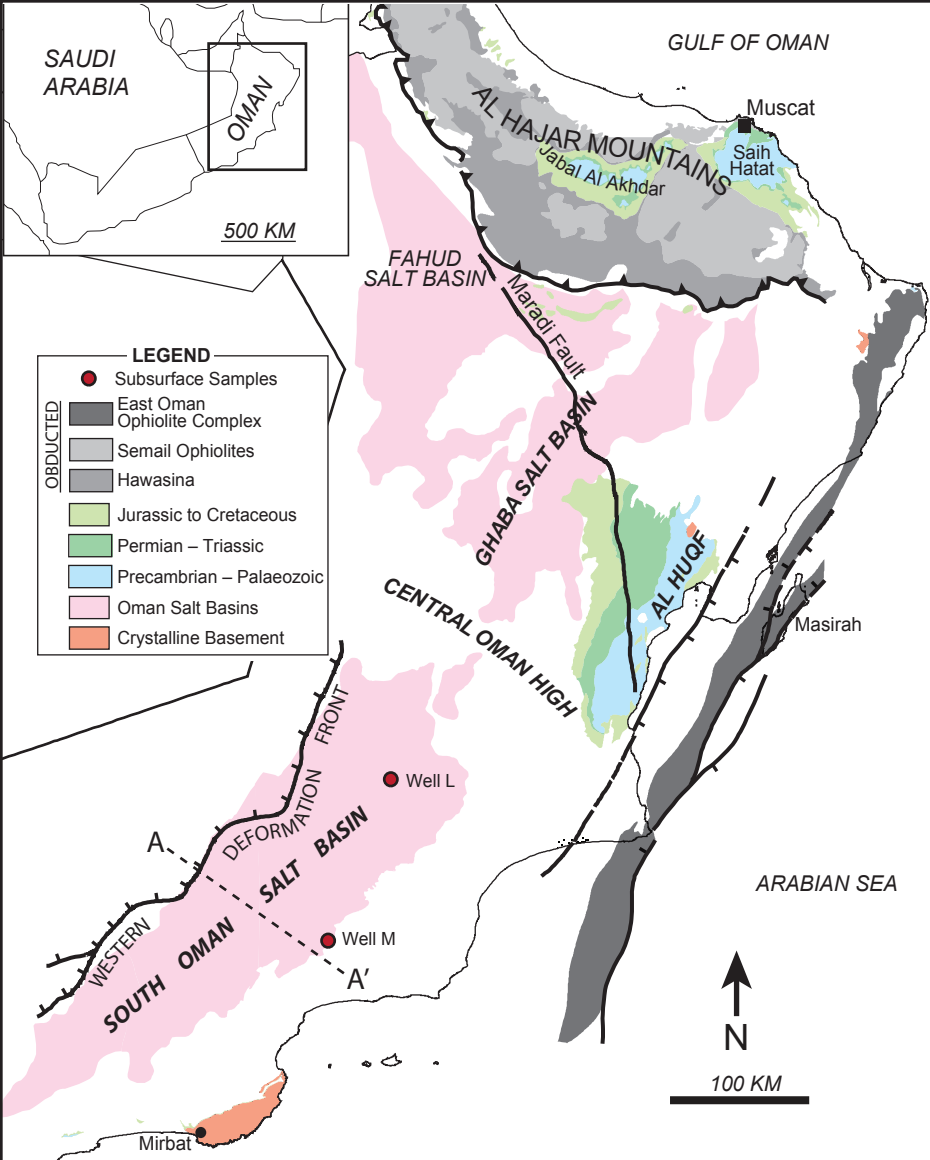
## Supplementary Information References

1. Fike, D. A., Grotzinger, J. P., Pratt, L. M. & Summons, R. E. Oxidation of the Ediacaran ocean. *Nature* **444**, 744–747 (2006).
2. Le Guerroué, E., Allen, P. A. & Cozzi, A. Chemostratigraphic and sedimentological framework of the largest negative carbon isotopic excursion in earth history: The neoproterozoic Shuram formation (Nafun Group, Oman). *Precambrian Res.* **146**, 68–92 (2006).
3. Cozzi, A., Allen, P. A. & Grotzinger, J. P. Understanding carbonate ramp dynamics using d<sup>13</sup>C profiles: Examples from the Neoproterozoic Buah Formation of Oman. *Terra Nov.* **16**, 62–67 (2004).
4. Le Guerroué, E., Allen, P. A. & Cozzi, A. Parasequence development in the Ediacaran Shuram Formation (Nafun Group, Oman): High-resolution stratigraphic test for primary origin of negative carbon isotopic ratios. *Basin Res.* **18**, 205–219 (2006).
5. Grosjean, E., Love, G. D., Stalvies, C., Fike, D. A. & Summons, R. E. Origin of petroleum in the Neoproterozoic-Cambrian South Oman Salt Basin. *Org. Geochem.* **40**, 87–110 (2009).
6. Grosjean, E., Love, G. D., Kelly, A. E., Taylor, P. N. & Summons, R. E. Geochemical evidence for an Early Cambrian origin of the ‘Q’ oils and some condensates from north Oman. *Org. Geochem.* **45**, 77–90 (2012).
7. Love, G. D. *et al.* Fossil steroids record the appearance of Demospongiae during the Cryogenian period. *Nature* **457**, 718–21 (2009).
8. Nicholas, C. J. & Gold, S. E. P. Ediacaran – Cambrian Sirab Formation of the Al Huqf region, Sultanate of Oman. *GeoArabia* **17**, 49–98 (2012).
9. Bergmann, K. D. Constraints on the carbon cycle and climate during the early evolution of animals. (California Institute of Technology, 2013).
10. Osburn, M. R., Owens, J., Bergmann, K. D. & Lyons, T. W. Dynamic changes in sulfate sulfur isotopes preceding the Ediacaran Shuram Excursion. *Geochim. Cosmochim. Acta* (2015).
11. Osburn, M., Grotzinger, J. & Bergmann, K. Facies, stratigraphy, and evolution of a middle ediacaran carbonate ramp: Khufai formation, sultanate of Oman. *Am. Assoc. Pet. Geol. Bull.* **98**, 1631–1667 (2014).
12. Lee, C., Love, G. D., Fischer, W. W., Grotzinger, J. P. & Halverson, G. P. Marine organic matter cycling during the Ediacaran Shuram excursion. *Geology* **43**, 1103–1106 (2015).
13. Le Guerroué, E. Duration and synchronicity of the largest negative carbon isotope excursion on Earth: The Shuram/Wonoka anomaly. *Comptes Rendus - Geosci.* **342**, 204–214 (2010).
14. Stolper, D. A. *et al.* Paleoecology and paleoceanography of the Athel silicilite, Ediacaran-Cambrian boundary, Sultanate of Oman. *Geobiology* **15**, 401–426 (2017).
15. Bergmann, K. D., Al Balushi, S. A. K., Mackey, T. J., Grotzinger, J. P. & Eiler, J. M. A 600-Million-Year Carbonate Clumped-Isotope Record from the Sultanate of Oman. *J. Sediment. Res.* **88**, 960–979 (2018).

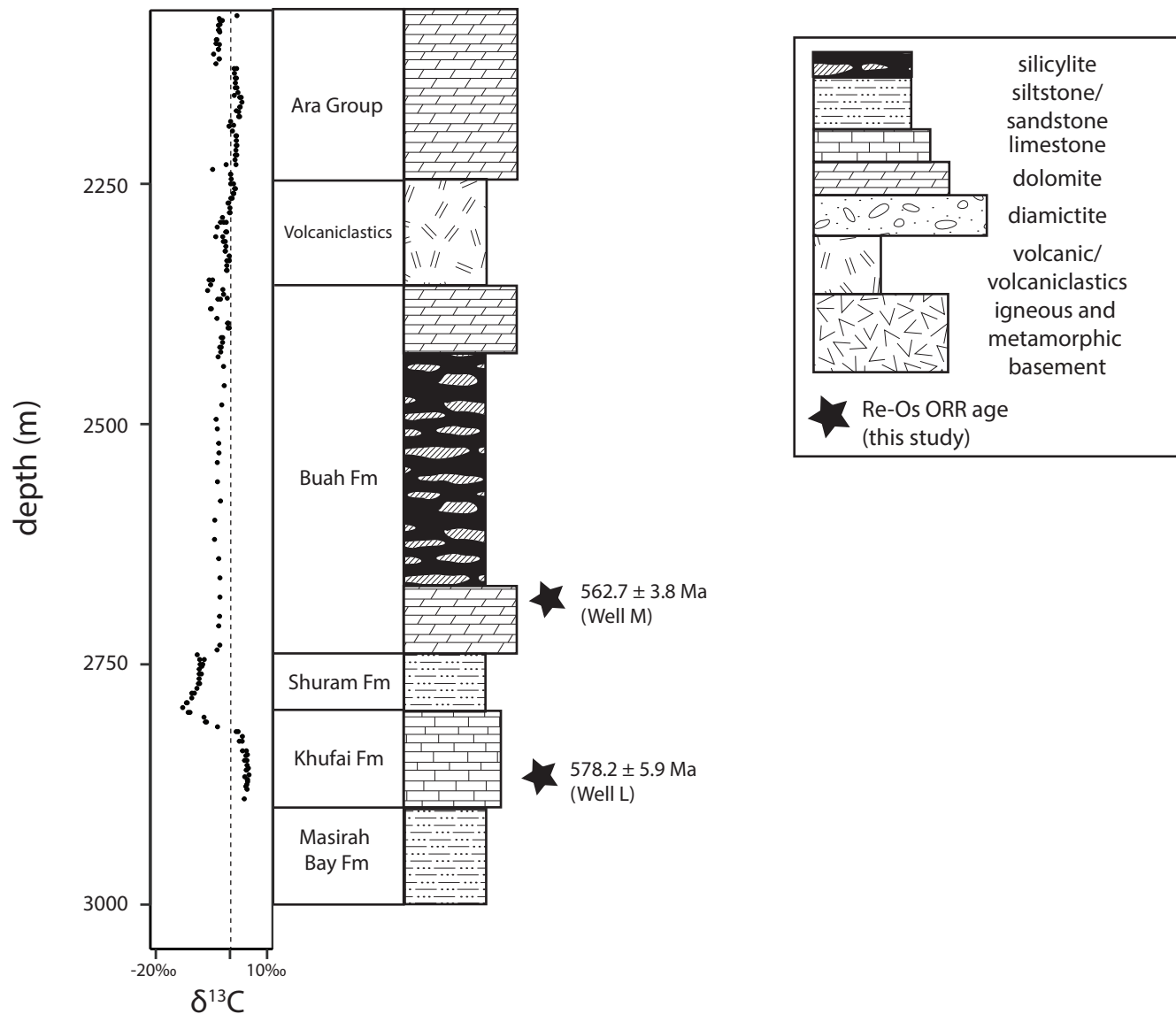
16. Forbes, G. A., Jansen, H. S. M. & Schreurs, J. *Lexicon of Oman: Subsurface Stratigraphy: reference guide to the stratigraphy of Oman's hydrocarbon basins*. (Gulf PetroLink, 2010).
17. Bowring, S. A. *et al.* Geochronologic constraints on the chronostratigraphic framework of the neoproterozoic Huqf Supergroup, Sultanate of Oman. *Am. J. Sci.* **307**, 1097–1145 (2007).
18. Allen, P. A. The Huqf Supergroup of Oman: Basin development and context for Neoproterozoic glaciation. *Earth-Science Rev.* **84**, 139–185 (2007).
19. Burns, S. J. & Matter, A. Carbon isotopic record of the latest Proterozoic from Oman. *Eclogae Geol. Helv.* **86**, 595–607 (1993).
20. Amthor, J. E. *et al.* Extinction of Cloudina and Namacalathus at the Precambrian-Cambrian boundary in Oman. *Geology* **31**, 431–434 (2003).
21. McCarron, M. E. G. The sedimentology and chemostratigraphy of the Nafun Group, Huqf Supergroup, Oman. (Oxford University, 1999).
22. Leather, J., Allen, P. A., Brasier, M. D. & Cozzi, A. Neoproterozoic snowball Earth under scrutiny: Evidence from the Fiq glaciation of Oman. *Geology* **30**, 891–894 (2002).
23. Cozzi, A., Grotzinger, J. P. & Allen, P. A. Evolution of a terminal Neoproterozoic carbonate ramp system (Buah Formation, Sultanate of Oman): Effects of basement paleotopography. *Bull. Geol. Soc. Am.* **116**, 1367–1384 (2004).
24. Gabrielse, H., Blusson, S. L. & Roddick, J. A. *Geology of Flat River, Glacier Lake, and Wrigley Lake map-areas, District of Mackenzie and Yukon Territory*. (Dept. of Energy, Mines, and Resources, 1972).
25. Narbonne, G. M. & Aitken, J. D. Neoproterozoic of the Mackenzie Mountains, northwest Canada. *Precambrian Res.* **73**, 101–121 (1995).
26. Strauss, J. V. *et al.* *Geological map of the Coal Creek inlier, Ogilvie Mountains (NTS 116B/10-15 and 116C/9, 16)*. (2014).
27. Moynihan, D. P., Strauss, J. V., Nelson, L. L. & Padgett, C. D. Upper Windermere Supergroup and the transition from rifting to continent-margin sedimentation, Nadaleen River area, northern Canadian Cordillera. *GSA Bull.* 1–29 (2019). doi:10.1130/b32039.1
28. Macdonald, F. A. *et al.* The stratigraphic relationship between the Shuram carbon isotope excursion, the oxygenation of Neoproterozoic oceans, and the first appearance of the Ediacara biota and bilaterian trace fossils in northwestern Canada. *Chem. Geol.* **362**, 250–272 (2013).
29. Aitken, J. D. *Uppermost Proterozoic formations in central Mackenzie Mountains, Northwest Territories*. **368**, (1989).
30. Cecile, M. P. *Geology of the northeastern Niddery Lake map area, east-central Yukon and adjacent Northwest Territories*. **553**, (2000).
31. Rooney, A. D., Strauss, J. V., Brandon, A. D. & Macdonald, F. A. A Cryogenian chronology: Two long-lasting synchronous neoproterozoic glaciations. *Geology* **43**, 459–462 (2015).
32. Aitken, J. D. Two Late Proterozoic glaciations, Mackenzie Mountains, northwestern Canada. *Geology* **19**, 445–448 (1991).
33. Hoffman, P. F., Kaufman, A. J., Halverson, G. P. & Schrag, D. P. A Neoproterozoic Snowball Earth. *Science (80-.)* **281**, 1342–1346 (1998).
34. James, N. P., Narbonne, G. M. & Kyser, T. K. Late Neoproterozoic cap carbonates: Mackenzie Mountains, northwestern Canada: precipitation and global glacial meltdown.

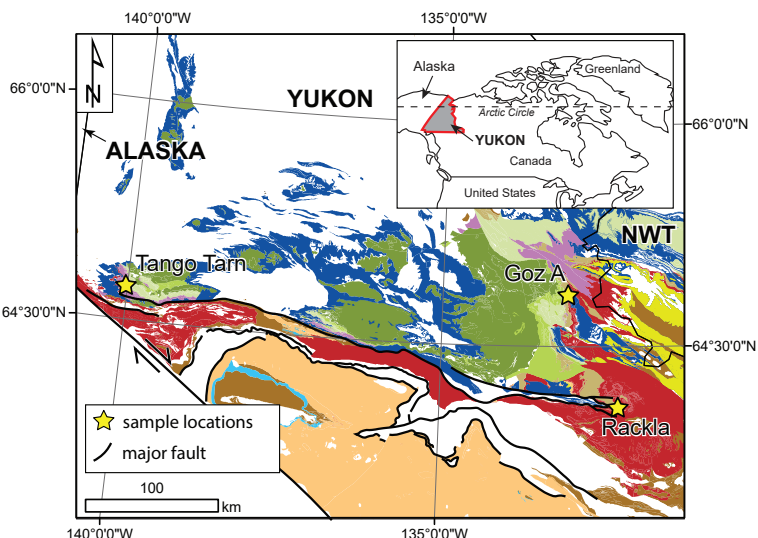
- Can. J. Earth Sci.* **38**, 1229–1262 (2001).
35. Narbonne, G. M., Kaufman, A. J. & Knoll, A. H. Integrated chemostratigraphy and biostratigraphy of the Windermere Supergroup, northwestern Canada: implications for Neoproterozoic correlations and the early evolution of animals. *Geol. Soc. Am. Bull.* **106**, 1281–1292 (1994).
  36. Kaufman, A. J., Knoll, A. H. & Narbonne, G. M. Isotopes, ice ages, and terminal Proterozoic earth history. *Proc. Natl. Acad. Sci.* **94**, 6600–6605 (1997).
  37. Carbone, C. A. & Narbonne, G. M. When life got smart: the evolution of behavioral complexity through the Ediacaran and early Cambrian of NW Canada. *J. Paleontol.* **88**, 309–330 (2014).
  38. Mustard, P. S., Donaldson, J. A. & Thompson, R. I. Trace fossils and stratigraphy of the Precambrian–Cambrian boundary sequence, upper Harper group, Ogilvie Mountains, Yukon. in *Current Research, Part E: Geological Survey of Canada Paper* 197–203 (1988).
  39. Strauss, J. V., Rooney, A. D., MacDonald, F. A., Brandon, A. D. & Knoll, A. H. 740 Ma vase-shaped microfossils from Yukon, Canada: Implications for neoproterozoic chronology and biostratigraphy. *Geology* **42**, 659–662 (2014).
  40. Thompson, R. I., Mustard, P. S. & Roots. *Geology of the Dawson map area (NTS116B, C)(northeast of Tintina trench)*. (1994).
  41. Mustard, P. S. & Roots, C. F. *Rift-related volcanism, sedimentation, and tectonic setting of the Mount Harper Group, Ogilvie Mountains, Yukon Territory*. (1997).
  42. Kendall, B., Creaser, R. A. & Selby, D.  $^{187}\text{Re} - ^{187}\text{Os}$  geochronology of Precambrian organic-rich sedimentary rocks. in *Global Neoproterozoic Petroleum Systems: The Emerging Potential in North Africa* (eds. Craig, J., Thurow, J., Thusu, B., Whitman, A. & Abutarruma, Y.) 85–107 (Geological Society, 2009).
  43. Selby, D. & Creaser, R. A. Re-Os geochronology of organic rich sediments: An evaluation of organic matter analysis methods. *Chem. Geol.* **200**, 225–240 (2003).
  44. Cumming, V. M., Poulton, S. W., Rooney, A. D. & Selby, D. Anoxia in the terrestrial environment during the late Mesoproterozoic. *Geology* **41**, 583–586 (2013).
  45. Cohen, A. S. & Waters, F. G. Separation of osmium from geological materials by solvent extraction for analysis by thermal ionisation mass spectrometry. *Anal. Chim. Acta* **2670**, 269–275 (1996).
  46. Birck, J. L. & Barman, M. R. Re-Os Isotopic Measurements at the Femtomole Level in Natural Samples. **20**, (1991).
  47. Kendall, B. S., Creaser, R. A., Ross, G. M. & Selby, D. Constraints on the timing of Marinoan “Snowball Earth” glaciation by  $^{187}\text{Re} - ^{187}\text{Os}$  dating of a Neoproterozoic, post-glacial black shale in Western Canada. *Earth Planet. Sci. Lett.* **222**, 729–740 (2004).
  48. Rooney, A. D., Chew, D. M. & Selby, D. Re–Os geochronology of the Neoproterozoic – Cambrian Dalradian Supergroup of Scotland and Ireland: Implications for Neoproterozoic stratigraphy, glaciations and Re–Os systematics. *Precambrian Res.* **185**, 202–214 (2011).
  49. Creaser, R. A., Papanastassiou, D. A. & Wasserburg, G. J. Negative thermal ion mass spectrometry of osmium, rhenium and iridium. *Geochim. Cosmochim. Acta* **55**, 397–401 (1991).
  50. Volkering, J., Walczyk, T. & Heumann, K. G. Osmium isotope ratio determinations by negative thermal ionization mass spectrometry. *Int. J. Mass Spectrom. Ion Process.* **105**, 147–159 (1991).

51. Luguet, A., Nowell, G. M. & Pearson, D. G. 184Os/188 Os and 186Os/188Os measurements by Negative Thermal Ionisation Mass Spectrometry (N-TIMS): Effects of interfering element and mass fractionation corrections on data accuracy and precision. *Geochimica et Cosmochimica Acta* **248**, 342–362 (2008).
52. Liu, J. & Pearson, D. G. Rapid, precise and accurate Os isotope ratio measurements of nanogram to sub-nanogram amounts using multiple Faraday collectors and amplifiers equipped with  $10\ 12\ \Omega$  resistors by N-TIMS. *Chem. Geol.* **363**, 301–311 (2014).
53. Gramlich, J. W., Murphy, T. J., Garner, E. L. & Shields, W. R. Absolute Isotopic Abundance Ratio and Atomic Weight of a Reference Sample of Rhenium. *J. Res. Natl. Bur. Stand. Phys. Chem.* **77A**, 691–698 (1973).
54. Smoliar, M., Walker, R. J. & Morgan, J. W. Re-Os Ages of Group IIA, IIIA, IVA, and IVB Iron Meteorites. *Science (80-. ).* **271**, (1996).
55. Ludwig, K. R. Calculation of uncertainties of U-Pb isotope data. *Earth Planet. Sci. Lett.* **46**, 212–220 (1980).
56. Ludwig, K. R. *Isoplot version 4.15: a geochronological toolkit for microsoft Excel.* (2008).
57. Boggiani, P. C. *et al.* Chemostratigraphy of the Tamengo Formation (Corumbá Group, Brazil): A contribution to the calibration of the Ediacaran carbon-isotope curve. *Precambrian Res.* **182**, 382–401 (2010).
58. Saylor, B. Z., Kaufman, A. J., Grotzinger, J. P. & Urban, F. A composite reference section for terminal proterozoic strata of southern Namibia. *J. Sediment. Res. A. Sediment. Petrol. Process.* **68**, 1223–1235 (1998).
59. Tahata, M. *et al.* Carbon and oxygen isotope chemostratigraphies of the Yangtze platform, South China: Decoding temperature and environmental changes through the Ediacaran. *Gondwana Res.* **23**, 333–353 (2013).
60. Jiang, G., Kaufman, A. J., Christie-Blick, N., Zhang, S. & Wu, H. Carbon isotope variability across the Ediacaran Yangtze platform in South China: Implications for a large surface-to-deep ocean  $^{13}\text{C}$  gradient. *Earth Planet. Sci. Lett.* **261**, 303–320 (2007).
61. Kaufman, A. J., Jacobsen, S. B. & Knoll, A. H. The Vendian record of Sr and C isotopic variations in seawater: Implications for tectonics and paleoclimate. *Earth Planet. Sci. Lett.* **120**, (1993).
62. Pu, J. P. *et al.* Dodging snowballs: Geochronology of the Gaskiers glaciation and the first appearance of the Ediacaran biota. *Geology* **44**, 955–958 (2016).
63. Condon, D. *et al.* U-Pb Ages from the Neoproterozoic Doushantuo Formation, China. *Science (80-. ).* **308**, 95–98 (2005).
64. Linnemann, U. *et al.* New high - resolution age data from the Ediacaran – Cambrian boundary indicate rapid, ecologically driven onset of the Cambrian explosion. *Terra Nov.* (2019). doi:10.1111/ter.12368
65. Parry, L. A. *et al.* Ichnological evidence for meiofaunal bilaterians from the terminal Ediacaran and earliest Cambrian of Brazil. *Nat. Ecol. Evol.* **1**, 1455–1464 (2017).
66. Liu, P., Yin, C., Gao, L., Tang, F. & Chen, S. New material of microfossils from the Ediacaran Doushantuo Formation in the Zhangcunping area, Yichang, Hubei Province and its zircon SHRIMP U-Pb age. *Chinese Sci. Bull.* **54**, 1058–1064 (2009).
67. Schmitz, M. D. Radiometric ages used in GTS2012. in *The Geologic Time Scale 1045–1082* (Elsevier, 2012).

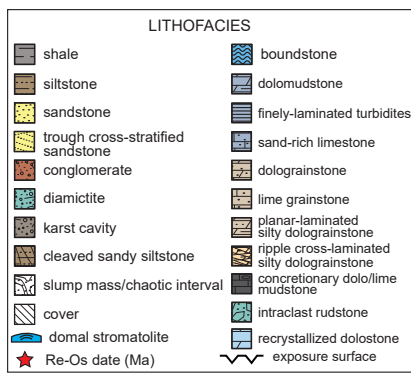


### Thamoud-6



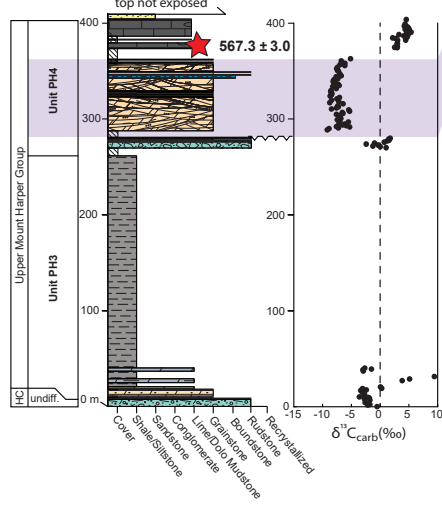


Proterozoic	Proterozoic-Terreneuvian Windermere Supergroup	Cambrian-Devonian Undivided
Mackenzie Mtns Supergroup (Tonian)	Rackla Group	Platformal carbonates
Pinguicula Group (Meso-Neoproterozoic)	Hay Creek Group	Transitional platform - basin
Wernecke Supergroup (Paleoproterozoic)	Hyland Group	Basinal carbonates
	Mount Harper, Rapitan Groups	Basinal siliciclastics



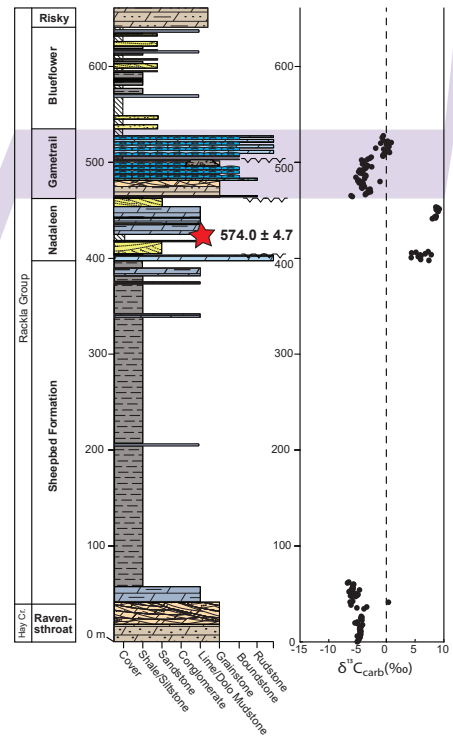
### Tango Tarn

J1713, JB1801, JB1704, J1711, F838 (Macdonald et al., 2013)



### Goz A

JB1707, T1701, J1719, T1703, F848, F849 (Macdonald et al., 2013)



### Rackla

Nadaleen Type Section, Section G3, Section B1 (Moynihan et al., 2019)

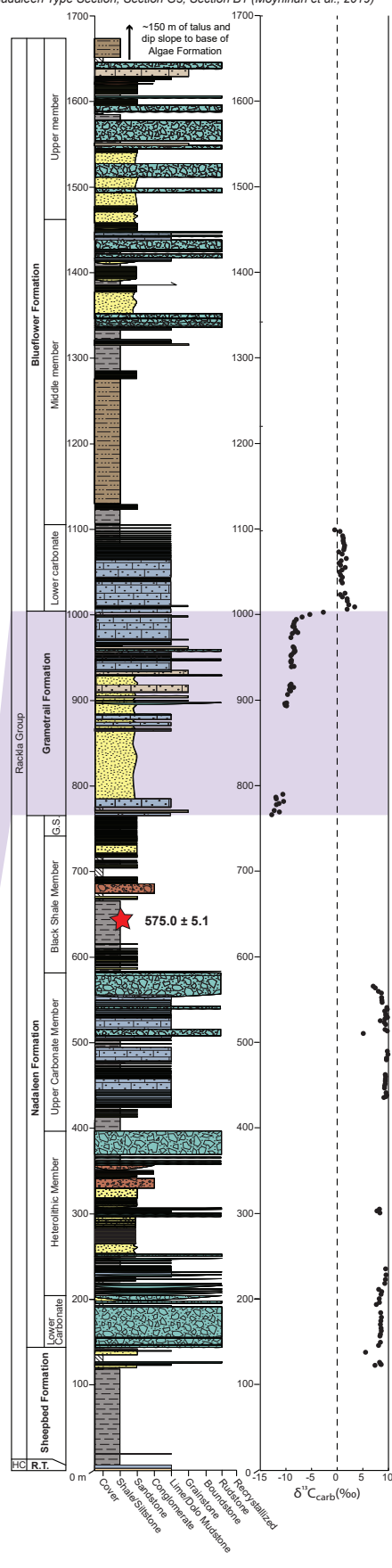


Table S1 Carbon Isotope Data

Region	Location	Stratigraphic Height (Outcrop) (m)	Depth (Drillcore) (m)	$\delta^{13}\text{C}_{\text{PDB}}\text{‰}$	Source	Unit	Age*	Note
<sup>a</sup> Ages in bold are tied directly to an age constraint or other assumption as detailed in the Note. Ages not in bold are interpolated between them.								
Oman	Thamoud-6 core	n/a	2074.00	-2.23 Petroleum Development Oman	Ara Group		537.73	
Oman	Thamoud-6 core	n/a	2075.00	-1.88 Petroleum Development Oman	Ara Group		537.79	
Oman	Thamoud-6 core	n/a	2079.00	-1.82 Petroleum Development Oman	Ara Group		537.87	
Oman	Thamoud-6 core	n/a	2080.00	-2.69 Petroleum Development Oman	Ara Group		538.08	
Oman	Thamoud-6 core	n/a	2080.00	-2.06 Petroleum Development Oman	Ara Group		538.09	
Oman	Thamoud-6 core	n/a	2080.00	-2.06 Petroleum Development Oman	Ara Group		538.32	
Oman	Thamoud-6 core	n/a	2085.00	-3.08 Petroleum Development Oman	Ara Group		538.38	
Oman	Thamoud-6 core	n/a	2090.00	-3.07 Petroleum Development Oman	Ara Group		538.67	
Oman	Thamoud-6 core	n/a	2090.00	-2.89 Petroleum Development Oman	Ara Group		538.67	
Oman	Thamoud-6 core	n/a	2090.00	-2.89 Petroleum Development Oman	Ara Group		538.78	
Oman	Thamoud-6 core	n/a	2100.00	-3.67 Petroleum Development Oman	Ara Group		539.25	
Oman	Thamoud-6 core	n/a	2100.00	-3.53 Petroleum Development Oman	Ara Group		539.25	
Oman	Thamoud-6 core	n/a	2100.00	-3.53 Petroleum Development Oman	Ara Group		539.48	
Oman	Thamoud-6 core	n/a	2105.00	-2.85 Petroleum Development Oman	Ara Group		539.54	
Oman	Thamoud-6 core	n/a	2110.00	-3.11 Petroleum Development Oman	Ara Group		539.83	
Oman	Thamoud-6 core	n/a	2110.00	-3.03 Petroleum Development Oman	Ara Group		539.83	
Oman	Thamoud-6 core	n/a	2115.00	-4.41 Petroleum Development Oman	Ara Group		540.13	
Oman	Thamoud-6 core	n/a	2120.00	-2.86 Petroleum Development Oman	Ara Group		540.42	
Oman	Thamoud-6 core	n/a	2120.00	-2.95 Petroleum Development Oman	Ara Group		540.42	
Oman	Thamoud-6 core	n/a	2125.00	-3.78 Petroleum Development Oman	Ara Group		540.71	
Oman	Thamoud-6 core	n/a	2130.00	-1.8 Petroleum Development Oman	Ara Group		541.00	
ID-TIMS U-Pb age on ash layer within A4C unit of Ara Group, sample BB-5, from Oman. Bowring et al. 2007. As recalculated in GTS 2012.								
Oman	Thamoud-6 core	n/a	2130.00	-1.13 Petroleum Development Oman	Ara Group	<b>541.09</b>		
Oman	Thamoud-6 core	n/a	2135.00	-1.21 Petroleum Development Oman	Ara Group	541.29		
Oman	Thamoud-6 core	n/a	2140.00	-1.73 Petroleum Development Oman	Ara Group	541.38		
Oman	Thamoud-6 core	n/a	2145.00	-1.47 Petroleum Development Oman	Ara Group	541.58		
Oman	Thamoud-6 core	n/a	2150.00	-1.42 Petroleum Development Oman	Ara Group	542.17		
Oman	Thamoud-6 core	n/a	2150.00	-2.15 Petroleum Development Oman	Ara Group	542.17		
Oman	Thamoud-6 core	n/a	2150.00	-1.16 Petroleum Development Oman	Ara Group	542.46		
Oman	Thamoud-6 core	n/a	2150.00	-2.66 Petroleum Development Oman	Ara Group	542.63		
Oman	Thamoud-6 core	n/a	2165.00	-2.32 Petroleum Development Oman	Ara Group	543.04		
Oman	Thamoud-6 core	n/a	2170.00	-2.65 Petroleum Development Oman	Ara Group	543.33		
Oman	Thamoud-6 core	n/a	2174.00	-1.73 Petroleum Development Oman	Ara Group	543.57		
Oman	Thamoud-6 core	n/a	2175.00	-2.35 Petroleum Development Oman	Ara Group	543.63		
Oman	Thamoud-6 core	n/a	2180.00	-2.6 Petroleum Development Oman	Ara Group	543.92		
Oman	Thamoud-6 core	n/a	2185.00	-0.17 Petroleum Development Oman	Ara Group	544.21		
Oman	Thamoud-6 core	n/a	2190.00	-0.24 Petroleum Development Oman	Ara Group	544.44		
Oman	Thamoud-6 core	n/a	2190.00	-0.21 Petroleum Development Oman	Ara Group	544.50		
Oman	Thamoud-6 core	n/a	2195.00	0.01 Petroleum Development Oman	Ara Group	544.79		
Oman	Thamoud-6 core	n/a	2200.00	-0.77 Petroleum Development Oman	Ara Group	545.08		
Oman	Thamoud-6 core	n/a	2200.00	-1.59 Petroleum Development Oman	Ara Group	545.08		
Oman	Thamoud-6 core	n/a	2205.00	-1.73 Petroleum Development Oman	Ara Group	545.37		
Oman	Thamoud-6 core	n/a	2210.00	-1.71 Petroleum Development Oman	Ara Group	545.57		
Oman	Thamoud-6 core	n/a	2215.00	-1.8 Petroleum Development Oman	Ara Group	545.96		
Oman	Thamoud-6 core	n/a	2220.00	-4.3 Petroleum Development Oman	Ara Group	546.25		
Oman	Thamoud-6 core	n/a	2220.00	-1.84 Petroleum Development Oman	Ara Group	546.25		
Oman	Thamoud-6 core	n/a	2225.00	-1.36 Petroleum Development Oman	Ara Group	546.54		
Oman	Thamoud-6 core	n/a	2230.00	-1.04 Petroleum Development Oman	Ara Group	546.83		
Oman	Thamoud-6 core	n/a	2230.00	-0.17 Petroleum Development Oman	Ara Group	547.12		
Oman	Thamoud-6 core	n/a	2240.00	-0.17 Petroleum Development Oman	Ara Group	547.42		
Oman	Thamoud-6 core	n/a	2240.00	-0.17 Petroleum Development Oman	Ara Group	547.42		
Oman	Thamoud-6 core	n/a	2245.00	0.34 Petroleum Development Oman	Ara Group	547.71		
Oman	Thamoud-6 core	n/a	2250.00	0.96 Petroleum Development Oman	Ara Group	548.00		
Estimated age of Bush-Ara unconformity, after Bowring et al. 2007.								
Oman	Thamoud-6 core	n/a	2250.00	0.19 Petroleum Development Oman	Ara Group	<b>541.09</b>		
Oman	Thamoud-6 core	n/a	2255.00	1.21 Petroleum Development Oman	Volcaniclastic	548.14		
Oman	Thamoud-6 core	n/a	2255.00	1.27 Petroleum Development Oman	Volcaniclastic	548.14		
Oman	Thamoud-6 core	n/a	2260.00	0.01 Petroleum Development Oman	Volcaniclastic	548.28		
Oman	Thamoud-6 core	n/a	2265.00	0.23 Petroleum Development Oman	Volcaniclastic	548.42		
Oman	Thamoud-6 core	n/a	2265.00	-0.54 Petroleum Development Oman	Volcaniclastic	548.43		
Oman	Thamoud-6 core	n/a	2270.00	-0.54 Petroleum Development Oman	Volcaniclastic	548.58		
Oman	Thamoud-6 core	n/a	2270.00	-0.39 Petroleum Development Oman	Volcaniclastic	548.58		
Oman	Thamoud-6 core	n/a	2275.00	-0.13 Petroleum Development Oman	Volcaniclastic	548.84		
Oman	Thamoud-6 core	n/a	2280.00	-0.03 Petroleum Development Oman	Volcaniclastic	548.84		
Oman	Thamoud-6 core	n/a	2280.00	-0.29 Petroleum Development Oman	Volcaniclastic	548.88		
Oman	Thamoud-6 core	n/a	2290.00	-2.54 Petroleum Development Oman	Volcaniclastic	549.12		
Oman	Thamoud-6 core	n/a	2290.00	-1.01 Petroleum Development Oman	Volcaniclastic	549.12		
Oman	Thamoud-6 core	n/a	2295.00	-0.23 Petroleum Development Oman	Volcaniclastic	549.25		
Oman	Thamoud-6 core	n/a	2300.00	-1.11 Petroleum Development Oman	Volcaniclastic	549.40		
Oman	Thamoud-6 core	n/a	2300.00	-0.89 Petroleum Development Oman	Volcaniclastic	549.40		
Oman	Thamoud-6 core	n/a	2305.00	-3.83 Petroleum Development Oman	Volcaniclastic	549.55		
Oman	Thamoud-6 core	n/a	2310.00	-1.77 Petroleum Development Oman	Volcaniclastic	549.65		
Oman	Thamoud-6 core	n/a	2310.00	-1.27 Petroleum Development Oman	Volcaniclastic	549.65		
Oman	Thamoud-6 core	n/a	2315.00	-1.23 Petroleum Development Oman	Volcaniclastic	549.83		
Oman	Thamoud-6 core	n/a	2320.00	-1.3 Petroleum Development Oman	Volcaniclastic	549.97		
Oman	Thamoud-6 core	n/a	2320.00	-0.13 Petroleum Development Oman	Volcaniclastic	549.97		
Oman	Thamoud-6 core	n/a	2325.00	-0.19 Petroleum Development Oman	Volcaniclastic	550.11		
Oman	Thamoud-6 core	n/a	2330.00	-0.84 Petroleum Development Oman	Volcaniclastic	550.25		
Oman	Thamoud-6 core	n/a	2330.00	-0.92 Petroleum Development Oman	Volcaniclastic	550.39		
Oman	Thamoud-6 core	n/a	2340.00	-0.78 Petroleum Development Oman	Volcaniclastic	550.53		
Oman	Thamoud-6 core	n/a	2340.00	-0.92 Petroleum Development Oman	Volcaniclastic	550.53		
Oman	Thamoud-6 core	n/a	2350.00	-5.61 Petroleum Development Oman	Volcaniclastic	550.81		
Oman	Thamoud-6 core	n/a	2350.00	-4.89 Petroleum Development Oman	Volcaniclastic	550.81		
Oman	Thamoud-6 core	n/a	2350.00	-5.21 Petroleum Development Oman	Volcaniclastic	550.95		
ID-TIMS U-Pb data on ash layer in Doushantu Fm. From Li & Condie et al. 2005. Associated with 373C values -0 permil, above Shuram.								
Excursion: sequence boundary between age and excursion in Doushantu stratigraphy. Correlated on the basis of chemostratigraphy. As recalculated in GTS 2012.								
Oman	Thamoud-6 core	n/a	2360.00	-1.92 Petroleum Development Oman	Bush Fm	<b>551.09</b>		
Oman	Thamoud-6 core	n/a	2361.00	-6.03 Petroleum Development Oman	Bush Fm	551.42		
Oman	Thamoud-6 core	n/a	2365.00	-1.73 Petroleum Development Oman	Bush Fm	552.75		
Oman	Thamoud-6 core	n/a	2365.00	-0.17 Petroleum Development Oman	Bush Fm	553.08		
Oman	Thamoud-6 core	n/a	2370.00	-0.25 Petroleum Development Oman	Bush Fm	554.41		
Oman	Thamoud-6 core	n/a	2370.00	-2.57 Petroleum Development Oman	Bush Fm	554.41		
Oman	Thamoud-6 core	n/a	2380.00	-5.27 Petroleum Development Oman	Bush Fm	557.72		
Oman	Thamoud-6 core	n/a	2380.00	-0.03 Petroleum Development Oman	Bush Fm	557.72		
Oman	Thamoud-6 core	n/a	2390.00	-3.51 Petroleum Development Oman	Bush Fm	561.04		
Well M sample, middle Bush Fm, Oman, this study. Sample Overides Shuram excursion; associated with positive 373C values.								
Oman	Thamoud-6 core	n/a	2390.00	-0.47 Petroleum Development Oman	Bush Fm	<b>562.32</b>		
Oman	Thamoud-6 core	n/a	2395.00	-0.84 Petroleum Development Oman	Bush Fm	562.79		
Oman	Thamoud-6 core	n/a	2400.00	-0.19 Petroleum Development Oman	Bush Fm	562.78		
Oman	Thamoud-6 core	n/a	2400.00	-1.96 Petroleum Development Oman	Bush Fm	562.93		
Oman	Thamoud-6 core	n/a	2410.00	-2.33 Petroleum Development Oman	Bush Fm	562.93		
Oman	Thamoud-6 core	n/a	2410.00	-2 Petroluem Development Oman	Bush Fm	563.00		
Oman	Thamoud-6 core	n/a	2420.00	-2.49 Petroleum Development Oman	Bush Fm	563.00		
Oman	Thamoud-6 core	n/a	2420.00	-0.13 Petroleum Development Oman	Bush Fm	563.15		
Oman	Thamoud-6 core	n/a	2425.00	-1.74 Petroleum Development Oman	Bush Fm	563.38		
Oman	Thamoud-6 core	n/a	2460.00	-1.55 Petroleum Development Oman	Bush Fm	563.68		
Oman	Thamoud-6 core	n/a	2460.00	-2.35 Petroleum Development Oman	Bush Fm	564.08		
Oman	Thamoud-6 core	n/a	2465.00	-1.73 Petroleum Development Oman	Bush Fm	564.21		
Oman	Thamoud-6 core	n/a	2505.00	-3.42 Petroleum Development Oman	Bush Fm	564.36		
Oman	Thamoud-6 core	n/a	2520.00	-3.03 Petroleum Development Oman	Bush Fm	564.59		
Oman	Thamoud-6 core	n/a	2520.00	-3.42 Petroleum Development Oman	Bush Fm	564.74		
Oman	Thamoud-6 core	n/a	2560.00	-3.37 Petroleum Development Oman	Bush Fm	564.89		
Oman	Thamoud-6 core	n/a	2600.00	-4.11 Petroleum Development Oman	Bush Fm	565.19		
Oman	Thamoud-6 core	n/a	2620.00	-1.47 Petroleum Development Oman	Bush Fm	565.79		
Oman	Thamoud-6 core	n/a	2640.00	-3.03 Petroleum Development Oman	Bush Fm	566.09		
Oman	Thamoud-6 core	n/a	2660.00	-2.71 Petroleum Development Oman	Bush Fm	566.40		
Oman	Thamoud-6 core	n/a	2680.00	-2.71 Petroleum Development Oman	Bush Fm	567.00		
Sample A1707, Blueflower Fm, NW Canada, this study. Lst 16 m above the contact with the underlying Gamelar Fm. Coal Creek location, lies in +2 permil plateau above a carbonate gap. Correlated to Oman on the basis of chemostratigraphy.								
Oman	Thamoud-6 core	n/a	2700.00	-3.8 Petroleum Development Oman	Shuram Fm	<b>567.88</b>		
Oman	Thamoud-6 core	n/a	2710.00	-3.03 Petroleum Development Oman	Shuram Fm	570.65		
Oman	Thamoud-6 core	n/a	2730.00	-2.74 Petroleum Development Oman	Shuram Fm	568.99		
Oman	Thamoud-6 core	n/a	2735.00	-3.48 Petroleum Development Oman	Shuram Fm	568.25		
Oman	Thamoud-6 core	n/a	2740.00	-3.48 Petroleum Development Oman	Shuram Fm	568.53		
Oman	Thamoud-6 core	n/a	2745.00	-6.94 Petroleum Development Oman	Shuram Fm	568.91		
Oman	Thamoud-6 core	n/a	2745.00	-8.16 Petroleum Development Oman	Shuram Fm	569.81		
Oman	Thamoud-6 core	n/a	2750.00	-7.32 Petroleum Development Oman	Shuram Fm	570.09		
Oman	Thamoud-6 core	n/a	2750.00	-7.02 Petroleum Development Oman	Shuram Fm	570.09		
Oman	Thamoud-6 core	n/a	2752.00	-7.58 Petroleum Development Oman	Shuram Fm	570.20		
Oman	Thamoud-6 core	n/a	2755.00	-8.28 Petroleum Development Oman	Shuram Fm	570.37		
Oman	Thamoud-6 core	n/a	2760.00	-8.27 Petroleum Development Oman	Shuram Fm	570.65		
Oman	Thamoud-6 core	n/a	2765.00	-8.31 Petroleum Development Oman	Shuram Fm	570.93		
Oman	Thamoud-6 core	n/a	2770.00	-8.49 Petroleum Development Oman	Shuram Fm	571.21		
Oman	Thamoud-6 core	n/a	2775.00	-8.92 Petroleum Development Oman	Shuram Fm	571.49		
Oman	Thamoud-6 core	n/a	2780.00	-10.28 Petroleum Development Oman	Shuram Fm	571.77		
Oman	Thamoud-6 core	n/a	2785.00	-10.31 Petroleum Development Oman	Shuram Fm	572.05		
Oman	Thamoud-6 core	n/a	2790.00	-11.53 Petroleum Development Oman	Shuram Fm	572.33		
Oman	Thamoud-6 core	n/a	2795.00	-12.75 Petroleum Development Oman	Shuram Fm	572.60		
Oman	Thamoud-6 core	n/a	2800.00	-10.78 Petroleum Development Oman	Khufai Fm	572.88		
Oman	Thamoud-6 core	n/a	2805.00	-11.02 Petroleum Development Oman	Khufai Fm	572.98		
Oman	Thamoud-6 core	n/a	2810.00	-7 Petroleum Development Oman	Khufai Fm	573.16		
Oman	Thamoud-6 core	n/a	2810.0					

Oman	Thamoud-6 core	n/a	2815	-3.36	Petroleum Development Oman	Khufai Fm	573.72	
Oman	Thamoud-6 core	n/a	2820	1.67	Petroleum Development Oman	Khufai Fm	574.08	Sample J17-9, Nadisien Fm, NW Canada.
Oman	Thamoud-6 core	n/a	2825	3.35	Petroleum Development Oman	Khufai Fm	574.26	Underlies Shurash excursion. Occurs within a
Oman	Thamoud-6 core	n/a	2830	2.52	Petroleum Development Oman	Khufai Fm	574.53	plateau δ <sup>13</sup> C values of +9 permille about 30
Oman	Thamoud-6 core	n/a	2835	3.39	Petroleum Development Oman	Khufai Fm	574.53	meters below contact with the Gametta.
Oman	Thamoud-6 core	n/a	2840	4.42	Petroleum Development Oman	Khufai Fm	575.05	Correlated to Oman on the basis of
Oman	Thamoud-6 core	n/a	2844	4.42	Petroleum Development Oman	Khufai Fm	575.26	574.1 chemostatigraphy.
Oman	Thamoud-6 core	n/a	2845	4.3	Petroleum Development Oman	Khufai Fm	575.31	
Oman	Thamoud-6 core	n/a	2850	3.93	Petroleum Development Oman	Khufai Fm	575.58	
Oman	Thamoud-6 core	n/a	2855	4.17	Petroleum Development Oman	Khufai Fm	575.84	
Oman	Thamoud-6 core	n/a	2858	4.96	Petroleum Development Oman	Khufai Fm	576.00	
Oman	Thamoud-6 core	n/a	2860	4.4	Petroleum Development Oman	Khufai Fm	576.10	
Oman	Thamoud-6 core	n/a	2865	4.5	Petroleum Development Oman	Khufai Fm	576.10	
Oman	Thamoud-6 core	n/a	2865	5.13	Petroleum Development Oman	Khufai Fm	576.38	
Oman	Thamoud-6 core	n/a	2867	3.98	Petroleum Development Oman	Khufai Fm	576.47	
Oman	Thamoud-6 core	n/a	2870	4.02	Petroleum Development Oman	Khufai Fm	576.63	
Oman	Thamoud-6 core	n/a	2870	4.72	Petroleum Development Oman	Khufai Fm	576.63	
Oman	Thamoud-6 core	n/a	2872	4.76	Petroleum Development Oman	Khufai Fm	576.73	
Oman	Thamoud-6 core	n/a	2875	4.54	Petroleum Development Oman	Khufai Fm	576.89	
Oman	Thamoud-6 core	n/a	2877	4.62	Petroleum Development Oman	Khufai Fm	576.89	
Oman	Thamoud-6 core	n/a	2880	4.61	Petroleum Development Oman	Khufai Fm	577.15	
Oman	Thamoud-6 core	n/a	2890	3.86	Petroleum Development Oman	Khufai Fm	577.68	
Oman	Thamoud-6 core	n/a	2900		Petroleum Development Oman	basal Khufai Fm		Wat L sample, basal Khufai Fm, Oman. This
Northwest Canada	Redstone section	0.0	n/a	-1.9	James et al. 2001	Ravensthorpe Fm	635.3	study. Undates Shurash excursion.
Northwest Canada	Redstone section	0.0	n/a	-0.7	James et al. 2001	Ravensthorpe Fm	635.3	ID-TIMS U-Pb date on ash layer in Doushantuo
Northwest Canada	Redstone section	0.1	n/a	-1.7	James et al. 2001	Ravensthorpe Fm	635.3	Fm, China. Condon et al. 2005. Correlated to the
Northwest Canada	Redstone section	0.2	n/a	-1.9	James et al. 2001	Ravensthorpe Fm	635.3	Northwest Canada cap carbonate. As
Northwest Canada	Redstone section	0.5	n/a	-2.3	James et al. 2001	Ravensthorpe Fm	635.3	635.3 recalculated in GTS 2012.
Northwest Canada	Redstone section	0.7	n/a	-2.0	James et al. 2001	Ravensthorpe Fm	635.3	
Northwest Canada	Redstone section	1.0	n/a	-2.0	James et al. 2001	Ravensthorpe Fm	635.3	
Northwest Canada	Redstone section	1.5	n/a	-3.0	James et al. 2001	Ravensthorpe Fm	635.2	
Northwest Canada	Redstone section	2.0	n/a	-2.7	James et al. 2001	Ravensthorpe Fm	635.2	
Northwest Canada	Redstone section	2.0	n/a	-2.6	James et al. 2001	Ravensthorpe Fm	635.2	
Northwest Canada	Redstone section	2.2	n/a	-2.7	James et al. 2001	Ravensthorpe Fm	635.2	
Northwest Canada	Redstone section	2.3	n/a	-2.7	James et al. 2001	Ravensthorpe Fm	635.2	
Northwest Canada	Redstone section	2.4	n/a	-2.6	James et al. 2001	Ravensthorpe Fm	635.2	
Northwest Canada	Redstone section	2.5	n/a	-2.8	James et al. 2001	Ravensthorpe Fm	635.2	
Northwest Canada	Redstone section	3.0	n/a	-2.9	James et al. 2001	Ravensthorpe Fm	635.2	
Northwest Canada	Redstone section	3.0	n/a	-2.5	James et al. 2001	Ravensthorpe Fm	635.2	
Northwest Canada	Redstone section	3.5	n/a	-3.1	James et al. 2001	Ravensthorpe Fm	635.2	
Northwest Canada	Redstone section	3.8	n/a	-2.9	James et al. 2001	Ravensthorpe Fm	635.2	
Northwest Canada	Redstone section	4.0	n/a	-2.8	James et al. 2001	Ravensthorpe Fm	635.2	
Northwest Canada	Redstone section	4.5	n/a	-2.9	James et al. 2001	Ravensthorpe Fm	635.2	
Northwest Canada	Redstone section	5.0	n/a	-2.9	James et al. 2001	Ravensthorpe Fm	635.2	
Northwest Canada	Redstone section	5.5	n/a	-2.7	James et al. 2001	Ravensthorpe Fm	635.2	
Northwest Canada	Redstone section	5.8	n/a	-2.7	James et al. 2001	Ravensthorpe Fm	635.2	
Northwest Canada	Redstone section	6.5	n/a	-2.9	James et al. 2001	Ravensthorpe Fm	635.2	
Northwest Canada	Redstone section	6.8	n/a	-2.7	James et al. 2001	Ravensthorpe Fm	635.2	
Northwest Canada	Redstone section	7.8	n/a	-2.8	James et al. 2001	Ravensthorpe Fm	635.2	
Northwest Canada	Redstone section	8.8	n/a	-2.8	James et al. 2001	Ravensthorpe Fm	635.2	
Northwest Canada	Redstone section	9.8	n/a	-2.9	James et al. 2001	Ravensthorpe Fm	635.2	
Northwest Canada	Redstone section	11.0	n/a	-2.9	James et al. 2001	Ravensthorpe Fm	635.2	
Northwest Canada	Redstone section	12.0	n/a	-3.1	James et al. 2001	Ravensthorpe Fm	635.1	
Northwest Canada	Redstone section	13.0	n/a	-3.0	James et al. 2001	Ravensthorpe Fm	635.1	
Northwest Canada	Redstone section	13.8	n/a	-3.2	James et al. 2001	Ravensthorpe Fm	635.1	
Northwest Canada	Redstone section	14.0	n/a	-3.2	James et al. 2001	Ravensthorpe Fm	635.1	
Northwest Canada	Redstone section	14.7	n/a	-3.2	James et al. 2001	Ravensthorpe Fm	635.1	
Northwest Canada	Redstone section	17.7	n/a	-2.9	James et al. 2001	Ravensthorpe Fm	635.1	
Northwest Canada	Redstone section	18.8	n/a	-5.5	James et al. 2001	Ravensthorpe Fm	635.1	
Northwest Canada	Redstone section	19.2	n/a	-4.1	James et al. 2001	Ravensthorpe Fm	635.1	
Northwest Canada	Redstone section	19.2	n/a	-5.5	James et al. 2001	Ravensthorpe Fm	635.1	
Northwest Canada	Redstone section	20.0	n/a	-5.2	James et al. 2001	Ravensthorpe Fm	635.1	
Northwest Canada	Redstone section	21.0	n/a	-5.2	James et al. 2001	Ravensthorpe Fm	635.1	
Northwest Canada	Redstone section	22.0	n/a	-4.4	James et al. 2001	Ravensthorpe Fm	635.0	
Northwest Canada	Redstone section	22.7	n/a	-4.1	James et al. 2001	Ravensthorpe Fm	635.0	
Northwest Canada	Redstone section	23.0	n/a	-5.1	James et al. 2001	Ravensthorpe Fm	635.0	
Northwest Canada	Redstone section	23.8	n/a	-4.9	James et al. 2001	Ravensthorpe Fm	635.0	
Northwest Canada	Redstone section	24.0	n/a	-5.4	James et al. 2001	Ravensthorpe Fm	635.0	
Northwest Canada	Redstone section	24.8	n/a	-4.6	James et al. 2001	Ravensthorpe Fm	635.0	
Northwest Canada	Redstone section	26.7	n/a	-3.6	James et al. 2001	Ravensthorpe Fm	635.0	
Northwest Canada	Nadaleen Type Section	121.50	n/a	7.31	Moynihan et al. 2019	Nadakeen Fm	595.0	635.0 Estimated end of cap carbonate deposition.
Northwest Canada	Nadaleen Type Section	122.40	n/a	6.51	Moynihan et al. 2019	Nadakeen Fm	595.0	Estimated start of Nadaleen Fm deposition on
Northwest Canada	Nadaleen Type Section	123.00	n/a	6.39	Moynihan et al. 2019	Nadakeen Fm	594.9	the basis of chemostatigraphic correlation.
Northwest Canada	Nadaleen Type Section	125.00	n/a	5.94	Moynihan et al. 2019	Nadakeen Fm	594.8	
Northwest Canada	Nadaleen Type Section	136.80	n/a	5.48	Moynihan et al. 2019	Nadakeen Fm	594.2	
Northwest Canada	Nadaleen Type Section	144.80	n/a	5.80	Moynihan et al. 2019	Nadakeen Fm	593.8	
Northwest Canada	Nadaleen Type Section	148.50	n/a	8.36	Moynihan et al. 2019	Nadakeen Fm	593.6	
Northwest Canada	Nadaleen Type Section	155.00	n/a	8.36	Moynihan et al. 2019	Nadakeen Fm	593.3	
Northwest Canada	Nadaleen Type Section	158.00	n/a	8.37	Moynihan et al. 2019	Nadakeen Fm	593.2	
Northwest Canada	Nadaleen Type Section	162.00	n/a	8.53	Moynihan et al. 2019	Nadakeen Fm	593.0	
Northwest Canada	Nadaleen Type Section	165.10	n/a	8.37	Moynihan et al. 2019	Nadakeen Fm	592.9	
Northwest Canada	Nadaleen Type Section	169.40	n/a	8.36	Moynihan et al. 2019	Nadakeen Fm	592.8	
Northwest Canada	Nadaleen Type Section	173.60	n/a	8.44	Moynihan et al. 2019	Nadakeen Fm	592.4	
Northwest Canada	Nadaleen Type Section	177.60	n/a	8.41	Moynihan et al. 2019	Nadakeen Fm	592.2	
Northwest Canada	Nadaleen Type Section	183.20	n/a	8.41	Moynihan et al. 2019	Nadakeen Fm	591.9	
Northwest Canada	Nadaleen Type Section	192.90	n/a	7.57	Moynihan et al. 2019	Nadakeen Fm	591.4	
Northwest Canada	Nadaleen Type Section	195.20	n/a	8.17	Moynihan et al. 2019	Nadakeen Fm	591.3	
Northwest Canada	Nadaleen Type Section	199.60	n/a	8.03	Moynihan et al. 2019	Nadakeen Fm	591.1	
Northwest Canada	Nadaleen Type Section	204.70	n/a	8.48	Moynihan et al. 2019	Nadakeen Fm	590.8	
Northwest Canada	Nadaleen Type Section	207.90	n/a	8.6	Moynihan et al. 2019	Nadakeen Fm	590.6	
Northwest Canada	Nadaleen Type Section	210.50	n/a	8.03	Moynihan et al. 2019	Nadakeen Fm	590.5	
Northwest Canada	Nadaleen Type Section	217.50	n/a	9.21	Moynihan et al. 2019	Nadakeen Fm	590.1	
Northwest Canada	Nadaleen Type Section	222.10	n/a	9.33	Moynihan et al. 2019	Nadakeen Fm	589.9	
Northwest Canada	Nadaleen Type Section	227.50	n/a	9.30	Moynihan et al. 2019	Nadakeen Fm	589.8	
Northwest Canada	Nadaleen Type Section	234.60	n/a	8.37	Moynihan et al. 2019	Nadakeen Fm	589.3	
Northwest Canada	Nadaleen Type Section	300.20	n/a	8.26	Moynihan et al. 2019	Nadakeen Fm	588.0	
Northwest Canada	Nadaleen Type Section	302.50	n/a	7.69	Moynihan et al. 2019	Nadakeen Fm	585.8	
Northwest Canada	Nadaleen Type Section	324.60	n/a	9.03	Moynihan et al. 2019	Nadakeen Fm	585.7	
Northwest Canada	Nadaleen Type Section	435.50	n/a	8.03	Moynihan et al. 2019	Nadakeen Fm	579.1	
Northwest Canada	Nadaleen Type Section	436.50	n/a	9.43	Moynihan et al. 2019	Nadakeen Fm	579.1	
Northwest Canada	Nadaleen Type Section	439.10	n/a	9.48	Moynihan et al. 2019	Nadakeen Fm	578.8	
Northwest Canada	Nadaleen Type Section	441.10	n/a	9.48	Moynihan et al. 2019	Nadakeen Fm	578.8	
Northwest Canada	Nadaleen Type Section	446.60	n/a	9.16	Moynihan et al. 2019	Nadakeen Fm	578.6	
Northwest Canada	Nadaleen Type Section	449.20	n/a	9.18	Moynihan et al. 2019	Nadakeen Fm	578.4	
Northwest Canada	Nadaleen Type Section	451.60	n/a	9.17	Moynihan et al. 2019	Nadakeen Fm	578.3	
Northwest Canada	Nadaleen Type Section	454.80	n/a	9.31	Moynihan et al. 2019	Nadakeen Fm	578.2	
Northwest Canada	Nadaleen Type Section	457.10	n/a	9.33	Moynihan et al. 2019	Nadakeen Fm	578.0	
Northwest Canada	Nadaleen Type Section	460.00	n/a	9.34	Moynihan et al. 2019	Nadakeen Fm	577.9	
Northwest Canada	Nadaleen Type Section	477.80	n/a	10.89	Moynihan et al. 2019	Nadakeen Fm	577.0	
Northwest Canada	Nadaleen Type Section	479.70	n/a	9.80	Moynihan et al. 2019	Nadakeen Fm	576.9	
Northwest Canada	Nadaleen Type Section	481.70	n/a	9.54	Moynihan et al. 2019	Nadakeen Fm	576.8	
Northwest Canada	Nadaleen Type Section	484.20	n/a	10.03	Moynihan et al. 2019	Nadakeen Fm	576.7	
Northwest Canada	Nadaleen Type Section	486.10	n/a	9.82	Moynihan et al. 2019	Nadakeen Fm	576.6	
Northwest Canada	Nadaleen Type Section	489.80	n/a	9.7	Moynihan et al. 2019	Nadakeen Fm	576.4	
Northwest Canada	Nadaleen Type Section	491.30	n/a	9.04	Moynihan et al. 2019	Nadakeen Fm	576.3	
Northwest Canada	Nadaleen Type Section	493.20	n/a	9.14	Moynihan et al. 2019	Nadakeen Fm	576.2	
Northwest Canada	Nadaleen Type Section	495.20	n/a	10.86	Moynihan et al. 2019	Nadakeen Fm	576.1	
Northwest Canada	Nadaleen Type Section	496.30	n/a	8.55	Moynihan et al. 2019	Nadakeen Fm	576.1	
Northwest Canada	Nadaleen Type Section	499.00	n/a	9.69	Moynihan et al. 2019	Nadakeen Fm	575.9	
Northwest Canada	Nadaleen Type Section	508.80	n/a	11.38	Moynihan et al. 2019	Nadakeen Fm	575.4	
Northwest Canada	Nadaleen Type Section	510.60	n/a	9.04	Moynihan et al. 2019	Nadakeen Fm	575.3	
Northwest Canada	Nadaleen Type Section	513.50	n/a	9.82	Moynihan et al. 2019	Nadakeen Fm	575.2	
Northwest Canada	Nadaleen Type Section	515.20	n/a	9.26	Moynihan et al. 2019	Nadakeen Fm	575.1	
Northwest Canada	Nadaleen Type Section	521.10	n/a	9.38	Moynihan et al. 2019	Nadakeen Fm	574.8	
Northwest Canada	Nadaleen Type Section	523.40	n/a	9.33	Moynihan et al. 2019	Nadakeen Fm	574.7	
Northwest Canada	Nadaleen Type Section	527.50	n/a	9.22	Moynihan et al. 2019	Nadakeen Fm	574.5	
Northwest Canada	Nadaleen Type Section	529.50	n/a	9.73	Moynihan et al. 2019	Nadakeen Fm	574.4	
Northwest Canada	Nadaleen Type Section	531.70	n/a	10.86	Moynihan et al. 2019	Nadakeen Fm	574.3	
Northwest Canada	Nadaleen Type Section	533.50	n/a	9.39	Moynihan et al. 2019	Nadakeen Fm	574.2	
Northwest Canada	Nadaleen Type Section	536.90	n/a	9.2	Moynihan et al. 2019	Nadakeen Fm	574.1	

nneumann et al. 2018), a combined paleontological study + ID-TIMS U-Pb ash dates from Swartpunt section, Namibia, suggest moving the Precambrian-Cambrian boundary younger, between 538.8 and 538.6 Ma.

Tied to age model built from Jang et al. 2007 data for boundary of Shibanian and Hansjin members.							
<b>547.29</b>							
China	Drill core	n/a	35.8	-1.87	Tahata et al. 2013	Dengying Fm	
China	Drill core	n/a	38.08	-0.32	Tahata et al. 2013	Dengying Fm	547.38
China	Drill core	n/a	41.06	1.15	Tahata et al. 2013	Dengying Fm	548.33
China	Drill core	n/a	41.15	1.7	Tahata et al. 2013	Dengying Fm	548.35
China	Drill core	n/a	41.2	1.5	Tahata et al. 2013	Dengying Fm	548.35
China	Drill core	n/a	41.21	1.87	Tahata et al. 2013	Dengying Fm	548.36
China	Drill core	n/a	41.25	2.07	Tahata et al. 2013	Dengying Fm	548.37
China	Drill core	n/a	41.28	2.08	Tahata et al. 2013	Dengying Fm	548.37
China	Drill core	n/a	44.67	4.66	Tahata et al. 2013	Dengying Fm	549.02
China	Drill core	n/a	46.05	2.82	Tahata et al. 2013	Dengying Fm	549.28
China	Drill core	n/a	49.61	1.83	Tahata et al. 2013	Dengying Fm	549.98
China	Drill core	n/a	50.6	2.04	Tahata et al. 2013	Dengying Fm	550.15
China	Drill core	n/a	52.61	1.64	Tahata et al. 2013	Dengying Fm	550.53
China	Drill core	n/a	52.92	1.4	Tahata et al. 2013	Dengying Fm	550.59
China	Drill core	n/a	53	0.74	Tahata et al. 2013	Dengying Fm	550.60
China	Drill core	n/a	54.6	-0.34	Tahata et al. 2013	Dengying Fm	550.91
China	Drill core	n/a	54.76	-1.05	Tahata et al. 2013	Dengying Fm	550.94
China	Drill core	n/a	55.34	-0.84	Tahata et al. 2013	Dengying Fm	551.05
China	Drill core	n/a	55.47	-0.66	Tahata et al. 2013	Dengying Fm	551.07
ID-TIMS U-Pb date on ash layer in Doushantu Fm, China. Average age of 513C values = 0 prior to Shibanian excursion sequence boundary between age and excursion in stratigraphy. Condon et al. 2005. As recalculated							
<b>551.09</b>							
in GTS 2012. 560.27							
Sample A1707, Blueflower Fm, NW Canada. Lies 16 m above the contact with the underlying Gasfield Fm. Coal Creek location lies in +2 sample points above a carbonate gap. Corrected to China on the basis of chemostratigraphy return to less negative 513C values) and existing age constraints.							
<b>567.3</b>							
China	Drill core	n/a	60.91	-4.98	Tahata et al. 2013	Doushantu Fm (Member IV)	567.53
China	Drill core	n/a	62	-7.27	Tahata et al. 2013	Doushantu Fm (Member IV)	567.54
China	Drill core	n/a	62.48	-7.88	Tahata et al. 2013	Doushantu Fm (Member IV)	567.54
China	Drill core	n/a	64.11	-7.81	Tahata et al. 2013	Doushantu Fm (Member IV)	567.79
China	Drill core	n/a	66.54	-7.88	Tahata et al. 2013	Doushantu Fm (Member IV)	568.47
China	Drill core	n/a	72.2	-8.01	Tahata et al. 2013	Doushantu Fm (Member IV)	569.03
China	Drill core	n/a	72.39	-7.87	Tahata et al. 2013	Doushantu Fm (Member IV)	569.08
China	Drill core	n/a	73.87	-7.93	Tahata et al. 2013	Doushantu Fm (Member IV)	569.29
China	Drill core	n/a	73.95	-6.74	Tahata et al. 2013	Doushantu Fm (Member IV)	569.30
China	Drill core	n/a	75.4	-6.17	Tahata et al. 2013	Doushantu Fm (Member IV)	569.52
China	Drill core	n/a	75.86	-6.82	Tahata et al. 2013	Doushantu Fm (Member IV)	569.59
China	Drill core	n/a	75.9	-8.19	Tahata et al. 2013	Doushantu Fm (Member IV)	569.60
China	Drill core	n/a	79.2	-8.19	Tahata et al. 2013	Doushantu Fm (Member IV)	569.95
China	Drill core	n/a	80.92	-6.11	Tahata et al. 2013	Doushantu Fm (Member IV)	570.37
China	Drill core	n/a	81.07	-6.96	Tahata et al. 2013	Doushantu Fm (Member IV)	570.39
China	Drill core	n/a	84.17	-6.77	Tahata et al. 2013	Doushantu Fm (Member IV)	570.85
China	Drill core	n/a	87.23	-6.07	Tahata et al. 2013	Doushantu Fm (Member IV)	571.33
China	Drill core	n/a	87.38	-8.04	Tahata et al. 2013	Doushantu Fm (Member IV)	571.36
China	Drill core	n/a	88.95	-8.9	Tahata et al. 2013	Doushantu Fm (Member IV)	571.86
China	Drill core	n/a	89.97	-8.9	Tahata et al. 2013	Doushantu Fm (Member IV)	571.75
China	Drill core	n/a	91.1	-8.99	Tahata et al. 2013	Doushantu Fm (Member IV)	571.93
China	Drill core	n/a	92.4	-8.82	Tahata et al. 2013	Doushantu Fm (Member IV)	572.13
China	Drill core	n/a	93.5	-8.17	Tahata et al. 2013	Doushantu Fm (Member IV)	572.15
China	Drill core	n/a	93.65	-8.94	Tahata et al. 2013	Doushantu Fm (Member IV)	572.32
China	Drill core	n/a	94.81	-9	Tahata et al. 2013	Doushantu Fm (Member IV)	572.50
China	Drill core	n/a	95	-8.47	Tahata et al. 2013	Doushantu Fm (Member IV)	572.67
China	Drill core	n/a	95.44	-7.78	Tahata et al. 2013	Doushantu Fm (Member IV)	572.74
China	Drill core	n/a	97.19	-8.38	Tahata et al. 2013	Doushantu Fm (Member IV)	572.86
China	Drill core	n/a	97.33	-8.39	Tahata et al. 2013	Doushantu Fm (Member IV)	572.88
China	Drill core	n/a	97.47	-8.39	Tahata et al. 2013	Doushantu Fm (Member IV)	572.93
China	Drill core	n/a	97.79	-7.76	Tahata et al. 2013	Doushantu Fm (Member IV)	572.95
China	Drill core	n/a	97.94	-8.11	Tahata et al. 2013	Doushantu Fm (Member IV)	572.97
China	Drill core	n/a	98.19	-8.33	Tahata et al. 2013	Doushantu Fm (Member IV)	573.01
China	Drill core	n/a	98.48	-8.3	Tahata et al. 2013	Doushantu Fm (Member IV)	573.08
China	Drill core	n/a	98.65	-8.56	Tahata et al. 2013	Doushantu Fm (Member IV)	573.08
China	Drill core	n/a	98.67	-8.67	Tahata et al. 2013	Doushantu Fm (Member IV)	573.09
China	Drill core	n/a	99	-7.32	Tahata et al. 2013	Doushantu Fm (Member IV)	573.14
China	Drill core	n/a	99.26	-7.73	Tahata et al. 2013	Doushantu Fm (Member IV)	573.18
China	Drill core	n/a	99.55	-7.58	Tahata et al. 2013	Doushantu Fm (Member IV)	573.22
China	Drill core	n/a	99.72	-7.21	Tahata et al. 2013	Doushantu Fm (Member IV)	573.25
China	Drill core	n/a	99.85	-7.21	Tahata et al. 2013	Doushantu Fm (Member IV)	573.27
China	Drill core	n/a	100.05	-7.15	Tahata et al. 2013	Doushantu Fm (Member IV)	573.30
China	Drill core	n/a	100.13	-7.15	Tahata et al. 2013	Doushantu Fm (Member IV)	573.31
China	Drill core	n/a	100.27	-6.75	Tahata et al. 2013	Doushantu Fm (Member IV)	573.33
China	Drill core	n/a	100.43	-6.5	Tahata et al. 2013	Doushantu Fm (Member IV)	573.36
China	Drill core	n/a	100.52	-6.48	Tahata et al. 2013	Doushantu Fm (Member IV)	573.37
China	Drill core	n/a	100.65	-6.32	Tahata et al. 2013	Doushantu Fm (Member IV)	573.39
China	Drill core	n/a	100.8	-7.32	Tahata et al. 2013	Doushantu Fm (Member IV)	573.41
China	Drill core	n/a	100.99	-7.28	Tahata et al. 2013	Doushantu Fm (Member IV)	573.44
China	Drill core	n/a	101.13	-6.97	Tahata et al. 2013	Doushantu Fm (Member IV)	573.46
China	Drill core	n/a	101.38	-6.97	Tahata et al. 2013	Doushantu Fm (Member IV)	573.50
China	Drill core	n/a	101.5	-5.7	Tahata et al. 2013	Doushantu Fm (Member IV)	573.52
China	Drill core	n/a	101.7	-5.2	Tahata et al. 2013	Doushantu Fm (Member IV)	573.55
China	Drill core	n/a	101.89	-5.52	Tahata et al. 2013	Doushantu Fm (Member IV)	573.58
China	Drill core	n/a	102.01	-5.25	Tahata et al. 2013	Doushantu Fm (Member IV)	573.60
China	Drill core	n/a	102.09	-4.99	Tahata et al. 2013	Doushantu Fm (Member IV)	573.61
China	Drill core	n/a	102.17	-5.04	Tahata et al. 2013	Doushantu Fm (Member IV)	573.62
China	Drill core	n/a	102.32	-4.37	Tahata et al. 2013	Doushantu Fm (Member IV)	573.65
China	Drill core	n/a	102.4	-4.1	Tahata et al. 2013	Doushantu Fm (Member IV)	573.69
China	Drill core	n/a	104.06	-0.31	Tahata et al. 2013	Doushantu Fm (Member IV)	573.91
Sample J1719, Nadaileen Fm, NW Canada, this study. Underlies Shuram excursion. Correlated to China on the basis of chemostratigraphy.							
<b>574</b>							
China	Drill core	n/a	104.63	-0.27	Tahata et al. 2013	Doushantu Fm (Member III)	574.01
China	Drill core	n/a	105.34	-0.93	Tahata et al. 2013	Doushantu Fm (Member III)	574.07
China	Drill core	n/a	107.4	0.93	Tahata et al. 2013	Doushantu Fm (Member III)	576.60
China	Drill core	n/a	108.12	0.95	Tahata et al. 2013	Doushantu Fm (Member III)	577.66
China	Drill core	n/a	109.54	2.31	Tahata et al. 2013	Doushantu Fm (Member III)	577.78
China	Drill core	n/a	109.57	0.95	Tahata et al. 2013	Doushantu Fm (Member III)	577.98
China	Drill core	n/a	109.97	3.05	Tahata et al. 2013	Doushantu Fm (Member III)	579.15
China	Drill core	n/a	111.54	4.34	Tahata et al. 2013	Doushantu Fm (Member III)	579.37
China	Drill core	n/a	111.83	4.34	Tahata et al. 2013	Doushantu Fm (Member III)	579.89
China	Drill core	n/a	112.53	4.47	Tahata et al. 2013	Doushantu Fm (Member III)	579.91
China	Drill core	n/a	112.56	4.39	Tahata et al. 2013	Doushantu Fm (Member III)	580.05
China	Drill core	n/a	112.76	4.39	Tahata et al. 2013	Doushantu Fm (Member III)	580.16
China	Drill core	n/a	112.8	4.42	Tahata et al. 2013	Doushantu Fm (Member III)	580.17
China	Drill core	n/a	113.57	4.83	Tahata et al. 2013	Doushantu Fm (Member III)	580.67
China	Drill core	n/a	114	4.62	Tahata et al. 2013	Doushantu Fm (Member III)	580.99
China	Drill core	n/a	114.18	4.58	Tahata et al. 2013	Doushantu Fm (Member III)	581.13
China	Drill core	n/a	114.49	4.84	Tahata et al. 2013	Doushantu Fm (Member III)	581.35
China	Drill core	n/a	114.58	4.11	Tahata et al. 2013	Doushantu Fm (Member III)	581.42
China	Drill core	n/a	114.8	4.76	Tahata et al. 2013	Doushantu Fm (Member III)	581.59
China	Drill core	n/a	114.97	4.76	Tahata et al. 2013	Doushantu Fm (Member III)	581.71
China	Drill core	n/a	115.11	4.54	Tahata et al. 2013	Doushantu Fm (Member III)	581.82
China	Drill core	n/a	115.25	4.54	Tahata et al. 2013	Doushantu Fm (Member III)	581.93
China	Drill core	n/a	115.39	4.96	Tahata et al. 2013	Doushantu Fm (Member III)	582.03
China	Drill core	n/a	115.58	4.4	Tahata et al. 2013	Doushantu Fm (Member III)	582.17
China	Drill core	n/a	115.63	4.73	Tahata et al. 2013	Doushantu Fm (Member III)	582.20
China	Drill core	n/a	115.84	4.52	Tahata et al. 2013	Doushantu Fm (Member III)	582.35
China	Drill core	n/a	116.21	4.58	Tahata et al. 2013	Doushantu Fm (Member III)	582.64
China	Drill core	n/a	116.43	4.44	Tahata et al. 2013	Doushantu Fm (Member III)	582.80
China	Drill core	n/a	116.62	4.6	Tahata et al. 2013	Doushantu Fm (Member III)	583.04
China	Drill core	n/a	116.76	4.15	Tahata et al. 2013	Doushantu Fm (Member III)	583.05
China	Drill core	n/a	116.87	4.27	Tahata et al. 2013	Doushantu Fm (Member III)	583.13
China	Drill core	n/a	117.02	5.45	Tahata et al. 2013	Doushantu Fm (Member III)	583.34
China	Drill core	n/a	117.21	5.45	Tahata et al. 2013	Doushantu Fm (Member III)	583.38
China	Drill core	n/a	117.34	4.54	Tahata et al. 2013	Doushantu Fm (Member III)	583.48
China	Drill core	n/a	117.93	4.88	Tahata et al. 2013	Doushantu Fm (Member III)	583.92
China	Drill core	n/a	118.24	5.12	Tahata et al. 2013	Doushantu Fm (Member III)	584.15
China	Drill core	n/a	118.4	5.24	Tahata et al. 2013	Doushantu Fm (Member III)	584.27
China	Drill core	n/a	118.54	5.24	Tahata et al. 2013	Doushantu Fm (Member III)	584.37
China	Drill core	n/a	118.66	4.98	Tahata et al. 2013	Doushantu Fm (Member III)	584.46
China	Drill core	n/a	118.84	4.89	Tahata et al. 2013	Doushantu Fm (Member III)	584.60
China	Drill core	n/a	119.08	5.21	Tahata et al. 2013	Doushantu Fm (Member III)	584.78
China	Drill core	n/a	119.49	5.08	Tahata et al. 2013	Doushantu Fm (Member III)	585.05
China	Drill core	n/a	119.63	5.08	Tahata et al. 2013	Doushantu Fm (Member III)	585.19
China	Drill core	n/a	119.75	4.95	Tahata et al. 2013	Doushantu Fm (Member III)	585.29
China	Drill core	n/a	119.89	4.95	Tahata et al. 2013	Doushantu Fm (Member III)	585.45
China	Drill core	n/a	120.17	4.72	Tahata et al. 2013	Doushantu Fm (Member III)	585.59
China	Drill core	n/a</td					



China	Drill core	n/a	280.42	-2.48	Tahata et al. 2013	Doushantu Fm (Member I, cap carbonate)	634.57
China	Drill core	n/a	280.48	-2.48	Tahata et al. 2013	Doushantu Fm (Member I, cap carbonate)	634.50
China	Drill core	n/a	280.53	-2.3	Tahata et al. 2013	Doushantu Fm (Member I, cap carbonate)	634.63
China	Drill core	n/a	280.57	-2.58	Tahata et al. 2013	Doushantu Fm (Member I, cap carbonate)	634.64
China	Drill core	n/a	280.66	-2.26	Tahata et al. 2013	Doushantu Fm (Member I, cap carbonate)	634.68
China	Drill core	n/a	280.89	-1.55	Tahata et al. 2013	Doushantu Fm (Member I, cap carbonate)	634.70
China	Drill core	n/a	281.74	-2.96	Tahata et al. 2013	Doushantu Fm (Member I, cap carbonate)	632.20
ID-TIMS U-Pb date on ash layer in Doushantu Fm, China, from the Nantuo diamictite Member (plagioclase). Condor et al. 2005. As identified at this layer by Jiang et al., 2007.							
China	Drill core	n/a	281.87	-3.5	Tahata et al. 2013	Doushantu Fm (Member I, cap carbonate)	635.26
recalculated in GTS 2012. Condor et al. 2005 U-Pb TIMS zircon age:							
China	Jinrunongwan	155.50	n/a	-5.09	Jiang et al. 2007	Doushantu Fm (Member IV)	551.09
China	Jinrunongwan	155.00	n/a	-1.9	Jiang et al. 2007	Doushantu Fm (Member IV)	551.05
China	Jinrunongwan	156.20	n/a	-1.75	Jiang et al. 2007	Dengying Fm	551.05
China	Jinrunongwan	156.40	n/a	-1.23	Jiang et al. 2007	Dengying Fm	551.03
China	Jinrunongwan	159.00	n/a	0.49	Jiang et al. 2007	Dengying Fm	550.98
China	Jinrunongwan	163.00	n/a	1.7	Jiang et al. 2007	Dengying Fm	550.63
China	Jinrunongwan	166.00	n/a	5.86	Jiang et al. 2007	Dengying Fm	550.45
China	Jinrunongwan	170.00	n/a	5.86	Jiang et al. 2007	Dengying Fm	550.20
China	Jinrunongwan	172.00	n/a	6.02	Jiang et al. 2007	Dengying Fm	550.08
China	Jinrunongwan	176.00	n/a	4.8	Jiang et al. 2007	Dengying Fm	549.83
China	Jinrunongwan	179.00	n/a	4.36	Jiang et al. 2007	Dengying Fm	549.85
China	Jinrunongwan	185.00	n/a	3.84	Jiang et al. 2007	Dengying Fm	549.47
China	Jinrunongwan	185.00	n/a	3.79	Jiang et al. 2007	Dengying Fm	549.28
China	Jinrunongwan	189.00	n/a	4.12	Jiang et al. 2007	Dengying Fm	549.04
China	Jinrunongwan	192.00	n/a	4.19	Jiang et al. 2007	Dengying Fm	548.85
China	Jinrunongwan	193.00	n/a	4.34	Jiang et al. 2007	Dengying Fm	548.67
China	Jinrunongwan	199.00	n/a	4.17	Jiang et al. 2007	Dengying Fm	548.42
China	Jinrunongwan	203.00	n/a	4.3	Jiang et al. 2007	Dengying Fm	548.18
China	Jinrunongwan	205.00	n/a	4.1	Jiang et al. 2007	Dengying Fm	548.06
China	Jinrunongwan	208.00	n/a	3.69	Jiang et al. 2007	Dengying Fm	547.87
China	Jinrunongwan	211.00	n/a	3.15	Jiang et al. 2007	Dengying Fm	547.69
China	Jinrunongwan	215.00	n/a	3.1	Jiang et al. 2007	Dengying Fm	547.44
China	Shipai section	217.00	n/a	3.95	Jiang et al. 2007	Dengying Fm	547.32
China	Shipai section	218.60	n/a	1.87	Jiang et al. 2007	Dengying Fm	547.29
China	Shipai section	229.80	n/a	2.82	Jiang et al. 2007	Dengying Fm	547.10
China	Shipai section	231.10	n/a	2.02	Jiang et al. 2007	Dengying Fm	546.99
China	Shipai section	253.80	n/a	0.879	Jiang et al. 2007	Dengying Fm	546.67
China	Shipai section	265.20	n/a	1.82	Jiang et al. 2007	Dengying Fm	546.47
China	Shipai section	281.00	n/a	4.01	Jiang et al. 2007	Dengying Fm	546.19
China	Shipai section	281.30	n/a	2.784	Jiang et al. 2007	Dengying Fm	546.19
China	Shipai section	288.40	n/a	2.007	Jiang et al. 2007	Dengying Fm	546.07
China	Shipai section	307.90	n/a	1.849	Jiang et al. 2007	Dengying Fm	545.72
China	Shipai section	321.20	n/a	2.02	Jiang et al. 2007	Dengying Fm	545.51
China	Shipai section	338.10	n/a	3.326	Jiang et al. 2007	Dengying Fm	545.19
China	Shipai section	345.00	n/a	4.118	Jiang et al. 2007	Dengying Fm	545.07
China	Shipai section	350.00	n/a	3.204	Jiang et al. 2007	Dengying Fm	544.97
China	Shipai section	356.20	n/a	3.244	Jiang et al. 2007	Dengying Fm	544.88
China	Shipai section	362.90	n/a	4.201	Jiang et al. 2007	Dengying Fm	544.76
China	Shipai section	367.30	n/a	4.016	Jiang et al. 2007	Dengying Fm	544.69
China	Shipai section	372.90	n/a	4.016	Jiang et al. 2007	Dengying Fm	544.58
China	Shipai section	378.20	n/a	3.279	Jiang et al. 2007	Dengying Fm	544.49
China	Shipai section	383.80	n/a	3.184	Jiang et al. 2007	Dengying Fm	544.39
China	Shipai section	390.90	n/a	3.036	Jiang et al. 2007	Dengying Fm	544.27
China	Shipai section	398.10	n/a	3.017	Jiang et al. 2007	Dengying Fm	544.14
China	Shipai section	403.00	n/a	3.02	Jiang et al. 2007	Dengying Fm	544.05
China	Shipai section	408.20	n/a	2.022	Jiang et al. 2007	Dengying Fm	543.98
China	Shipai section	414.20	n/a	4.76	Jiang et al. 2007	Dengying Fm	543.86
China	Shipai section	419.90	n/a	4.76	Jiang et al. 2007	Dengying Fm	543.76
China	Shipai section	424.40	n/a	3.013	Jiang et al. 2007	Dengying Fm	543.68
China	Shipai section	447.50	n/a	3.493	Jiang et al. 2007	Dengying Fm	543.27
China	Shipai section	456.70	n/a	2.42	Jiang et al. 2007	Dengying Fm	543.11
China	Shipai section	464.00	n/a	2.02	Jiang et al. 2007	Dengying Fm	542.99
China	Shipai section	470.00	n/a	2.08	Jiang et al. 2007	Dengying Fm	542.88
China	Shipai section	476.00	n/a	1.413	Jiang et al. 2007	Dengying Fm	542.77
China	Shipai section	482.20	n/a	1.52	Jiang et al. 2007	Dengying Fm	542.67
China	Shipai section	490.00	n/a	3.135	Jiang et al. 2007	Dengying Fm	542.53
China	Shipai section	497.60	n/a	2.994	Jiang et al. 2007	Dengying Fm	542.39
China	Shipai section	506.50	n/a	2.472	Jiang et al. 2007	Dengying Fm	542.24
China	Shipai section	515.60	n/a	2.027	Jiang et al. 2007	Dengying Fm	542.08
China	Shipai section	531.50	n/a	2.282	Jiang et al. 2007	Dengying Fm	541.80
China	Shipai section	545.20	n/a	2.733	Jiang et al. 2007	Dengying Fm	541.56
China	Shipai section	551.90	n/a	2.027	Jiang et al. 2007	Dengying Fm	541.44
China	Shipai section	558.20	n/a	1.552	Jiang et al. 2007	Dengying Fm	541.33
China	Shipai section	565.20	n/a	2.961	Jiang et al. 2007	Dengying Fm	541.21
China	Shipai section	572.00	n/a	2.85	Jiang et al. 2007	Dengying Fm	541.06
China	Shipai section	578.10	n/a	1.52	Jiang et al. 2007	Dengying Fm	540.98
China	Shipai section	584.30	n/a	1.85	Jiang et al. 2007	Dengying Fm	540.87
China	Shipai section	590.00	n/a	2.84	Jiang et al. 2007	Dengying Fm	540.77
China	Shipai section	594.00	n/a	2.02	Jiang et al. 2007	Dengying Fm	540.70
China	Shipai section	598.80	n/a	2.965	Jiang et al. 2007	Dengying Fm	540.62
China	Shipai section	603.80	n/a	2.791	Jiang et al. 2007	Dengying Fm	540.53
China	Shipai section	607.20	n/a	2.027	Jiang et al. 2007	Dengying Fm	540.47
China	Shipai section	612.30	n/a	1.13	Jiang et al. 2007	Dengying Fm	540.37
China	Shipai section	621.80	n/a	3.033	Jiang et al. 2007	Dengying Fm	540.21
China	Shipai section	643.00	n/a	3.02	Jiang et al. 2007	Dengying Fm	539.88
China	Shipai section	652.00	n/a	3.033	Jiang et al. 2007	Dengying Fm	539.68
China	Shipai section	661.00	n/a	2.873	Jiang et al. 2007	Dengying Fm	539.52
China	Shipai section	670.00	n/a	3.179	Jiang et al. 2007	Dengying Fm	539.37
China	Shipai section	678.00	n/a	2.02	Jiang et al. 2007	Dengying Fm	539.20
China	Shipai section	686.00	n/a	0.09	Jiang et al. 2007	Dengying Fm	539.08
China	Shipai section	694.20	n/a	-0.144	Jiang et al. 2007	Dengying Fm	538.94

Precambrian-Cambrian boundary, Age after  
Linnemann et al. 2018, a combined  
paleontological study + ID-TIMS U-Pb ash dates  
on Swartpunt section, Namibia, suggest moving  
the Precambrian-Cambrian boundary younger.

China	Shipai section	707.90	n/a	-0.576	Jiang et al. 2007	Dengying Fm	538.7
Tuff dated by TIMS, upper Bocaina Fm, Pará et al. 2017. Minimum depositional age for Tamengo Fm. Oceans below a small negative excursion.							

Brazil	Laginha Mine western base	0.00	n/a	-3.84	Bogiani et al. 2010	Tamengo Fm	555.19
Brazil	Laginha Mine western base	0.70	n/a	-3.23	Bogiani et al. 2010	Tamengo Fm	554.99
Brazil	Laginha Mine western base	2.10	n/a	-0.71	Bogiani et al. 2010	Tamengo Fm	554.57
Brazil	Laginha Mine western base	3.20	n/a	-0.21	Bogiani et al. 2010	Tamengo Fm	554.26
Brazil	Laginha Mine western base	4.80	n/a	-0.71	Bogiani et al. 2010	Tamengo Fm	553.82
Brazil	Laginha Mine western base	7.00	n/a	-0.56	Bogiani et al. 2010	Tamengo Fm	553.18
Brazil	Laginha Mine western base	8.30	n/a	-0.43	Bogiani et al. 2010	Tamengo Fm	552.82
Brazil	Laginha Mine western base	11.00	n/a	-0.29	Bogiani et al. 2010	Tamengo Fm	552.05
Brazil	Laginha Mine western base	12.40	n/a	-0.29	Bogiani et al. 2010	Tamengo Fm	551.86
Brazil	Laginha Mine western base	14.40	n/a	-0.21	Bogiani et al. 2010	Tamengo Fm	551.17
Brazil	Laginha Mine western base	15.50	n/a	-1.38	Bogiani et al. 2010	Tamengo Fm	547.45
Brazil	Laginha Mine western base	17.30	n/a	-0.95	Bogiani et al. 2010	Tamengo Fm	550.76
Brazil	Laginha Mine western base	19.20	n/a	-1.48	Bogiani et al. 2010	Tamengo Fm	550.26
Brazil	Laginha Mine western base	20.00	n/a	-1.02	Bogiani et al. 2010	Tamengo Fm	547.42
Brazil	Laginha Mine western base	20.40	n/a	-1.02	Bogiani et al. 2010	Tamengo Fm	547.08
Brazil	Laginha Mine western base	22.00	n/a	-1.07	Bogiani et al. 2010	Tamengo Fm	548.48
Brazil	Laginha Mine western base	23.30	n/a	-1.1	Bogiani et al. 2010	Tamengo Fm	548.56
Brazil	Laginha Mine western base	23.60	n/a	0.42	Bogiani et al. 2010	Tamengo Fm	548.46
Brazil	Laginha Mine western base	24.60	n/a	-1.02	Bogiani et al. 2010	Tamengo Fm	548.17
Brazil	Laginha Mine western base	25.60	n/a	-1.34	Bogiani et al. 2010	Tamengo Fm	547.88
Brazil	Laginha Mine western base	27.20	n/a	-1.35	Bogiani et al. 2010	Tamengo Fm	547.45
Brazil	Laginha Mine western base	27.30	n/a	4.59	Bogiani et al. 2010	Tamengo Fm	547.42
Brazil	Laginha Mine western base	28.50	n/a	-1.89	Bogiani et al. 2010	Tamengo Fm	547.08
Brazil	Laginha Mine western base	30.20	n/a	-1.1	Bogiani et al. 2010	Tamengo Fm	546.57
Brazil	Laginha Mine western base	31.50	n/a	-1.3	Bogiani et al. 2010	Tamengo Fm	546.23
Brazil	Laginha Mine western base	32.00	n/a	-0.36	Bogiani et al. 2010	Tamengo Fm	546.08
Brazil	Laginha Mine western base	33.00	n/a	-0.36	Bogiani et al. 2010	Tamengo Fm	545.79
Brazil	Laginha Mine western base	36.20	n/a	0.45	Bogiani et al. 2010	Tamengo Fm	544.88
Brazil	Laginha Mine western base	37.00	n/a	0.13	Bogiani et al. 2010	Tamengo Fm	544.64
Brazil	Laginha Mine western base	38.00	n/a	-0.21	Bogiani et al. 2010	Tamengo Fm	544.29
Brazil	Laginha Mine western base	39.40	n/a	-0.56	Bogiani et al. 2010	Tamengo Fm	543.98
Brazil	Laginha Mine western base	40.40	n/a	0.34	Bogiani et al. 2010	Tamengo Fm	543.68
Brazil	Laginha Mine western base	42.60	n/a	0.54	Bogiani et al. 2010	Tamengo Fm	543.07
Brazil	Laginha Mine western base	44.00	n/a	0.54	Bogiani et al. 2010	Tamengo Fm	542.65

Brazil	Laginha Mine western	45.00	n/a	1.87	Bogiani et al. 2010	Tamengo Fm	542.37





<tbl\_r cells="8" ix="5" max

Namibia	Southern sub-basin	958.00	n/a	1.8	Saylor et al. 1998, digitized from figure 2D	Spitzkopf Member	540.04
Namibia	Southern sub-basin	972.00	n/a	2.5	Saylor et al. 1998, digitized from figure 2D	Spitzkopf Member	540.00
Namibia	Southern sub-basin	989.00	n/a	2.1	Saylor et al. 1998, digitized from figure 2D	Spitzkopf Member	539.94
Namibia	Southern sub-basin	1009.00	n/a	2.1	Saylor et al. 1998, digitized from figure 2D	Spitzkopf Member	539.88
Namibia	Southern sub-basin	1022.00	n/a	1.8	Saylor et al. 1998, digitized from figure 2D	Spitzkopf Member	539.84
Namibia	Southern sub-basin	1033.00	n/a	1.8	Saylor et al. 1998, digitized from figure 2D	Spitzkopf Member	539.80
Namibia	Southern sub-basin	1055.00	n/a	1.5	Saylor et al. 1998, digitized from figure 2D	Spitzkopf Member	539.73
Namibia	Southern sub-basin	1063.00	n/a	2.1	Saylor et al. 1998, digitized from figure 2D	Spitzkopf Member	539.70
Namibia	Southern sub-basin	1077.00	n/a	1	Saylor et al. 1998, digitized from figure 2D	Spitzkopf Member	539.65
Namibia	Southern sub-basin	1088.00	n/a	1.5	Saylor et al. 1998, digitized from figure 2D	Spitzkopf Member	539.62
Namibia	Southern sub-basin	1114.00	n/a	1.8	Saylor et al. 1998, digitized from figure 2D	Spitzkopf Member	539.54
Namibia	Southern sub-basin	1186.00	n/a	1	Saylor et al. 1998, digitized from figure 2D	Spitzkopf Member	539.30
Namibia	Southern sub-basin	1197.00	n/a	2	Saylor et al. 1998, digitized from figure 2D	Spitzkopf Member	539.27
Namibia	Southern sub-basin	1204.00	n/a	1.6	Saylor et al. 1998, digitized from figure 2D	Spitzkopf Member	539.24
Namibia	Southern sub-basin	1276.00	n/a	1.2	Saylor et al. 1998, digitized from figure 2D	Spitzkopf Member	539.01
Namibia	Southern sub-basin	1295.00	n/a	-1	Saylor et al. 1998, digitized from figure 2D	Spitzkopf Member	538.99
Namibia	Southern sub-basin	1289.00	n/a	1	Saylor et al. 1998, digitized from figure 2D	Spitzkopf Member	538.97
Namibia	Southern sub-basin	1293.00	n/a	1.6	Saylor et al. 1998, digitized from figure 2D	Spitzkopf Member	538.95
Namibia	Southern sub-basin	1304.00	n/a	1	Saylor et al. 1998, digitized from figure 2D	Spitzkopf Member	538.92
Namibia	Southern sub-basin	1317.00	n/a	1.4	Saylor et al. 1998, digitized from figure 2D	Spitzkopf Member	538.87
Namibia	Southern sub-basin	1324.00	n/a	0.9	Saylor et al. 1998, digitized from figure 2D	Spitzkopf Member	538.85
Namibia	Southern sub-basin	1346.00	n/a	0.9	Saylor et al. 1998, digitized from figure 2D	Spitzkopf Member	538.78
Namibia	Southern sub-basin	1352.00	n/a	1.8	Saylor et al. 1998, digitized from figure 2D	Spitzkopf Member	538.75
Namibia	Southern sub-basin	1376.00	n/a	0	Saylor et al. 1998, digitized from figure 2D	Spitzkopf Member	538.68
Namibia	Southern sub-basin	1376.00	n/a	1.2	Saylor et al. 1998, digitized from figure 2D	Spitzkopf Member	538.66
Namibia	Southern sub-basin	1386.00	n/a	0.7	Saylor et al. 1998, digitized from figure 2D	Spitzkopf Member	538.65
Namibia	Southern sub-basin	1396.00	n/a	1.9	Saylor et al. 1998, digitized from figure 2D	Spitzkopf Member	538.62
Namibia	Southern sub-basin	1398.00	n/a	0.7	Saylor et al. 1998, digitized from figure 2D	Spitzkopf Member	538.61
Namibia	Southern sub-basin	1407.00	n/a	1.2	Saylor et al. 1998, digitized from figure 2D	Spitzkopf Member	538.58

n/a

Nomtsas Fm

Nomtsas Fm ash, Namibia, Southern subbasin,  
+2 013C permille plateau. Dated by U-Pb TIMS  
**\$38.58** on zircon by Linnemann et al. 2018

Table S2: Re and Os elemental abundance and isotopic composition data for isochron regressions

Sample	Isochron	Re (ng/g)	$\pm$	Os (pg/g)	$\pm$	$^{192}\text{Os}$ (pg/g)	$\pm$	$^{187}\text{Re}/^{188}\text{Os}$	$\pm$	$^{187}\text{Os}/^{188}\text{Os}$	$\pm$	$\rho\text{ho}^{\text{a}}$	$\text{Osi}^{\text{b}}$
30	Well L	41.345	0.118	909.1	9.3	239.8	1.8	342.9918	2.7299	4.4592	0.0570	0.543	1.140
31		159.444	0.393	3084.5	18.9	769.6	2.6	412.1811	1.7281	5.1469	0.0247	0.572	1.159
32		192.669	0.473	3625.8	22.5	896.0	3.1	427.7917	1.8078	5.2690	0.0258	0.573	1.130
28		163.530	0.400	2805.6	18.0	659.1	2.3	493.6122	2.0855	5.9341	0.0290	0.576	1.158
34		288.910	0.706	4805.7	31.8	1109.4	3.9	518.0780	2.2189	6.1712	0.0315	0.567	1.158
27		70.994	0.175	1128.5	7.6	253.7	0.9	556.7242	2.4284	6.5406	0.0333	0.584	1.163
29		260.549	0.636	3823.0	25.4	815.4	2.8	635.7007	2.6535	7.3007	0.0350	0.575	1.150
26		210.434	0.516	2880.3	20.6	583.7	2.1	717.1764	3.1518	8.0781	0.0424	0.579	1.139
A	A1707	1.397	0.005	160.7	0.8	59.2	0.3	46.9540	0.3075	1.0532	0.0080	0.590	0.608
B	64° 43' 10.0704" -140°	3.883	0.012	79.8	0.5	22.0	0.1	351.4028	1.9460	3.9508	0.0246	0.599	0.616
C	2'30.0834"	4.976	0.017	61.5	0.5	12.3	0.1	802.7904	5.4531	8.2357	0.0618	0.676	0.616
D		2.311	0.008	43.6	0.3	11.6	0.1	397.2155	2.9232	4.3846	0.0372	0.654	0.615
E		0.821	0.005	205.1	0.8	77.7	0.3	21.0201	0.1603	0.8132	0.0050	0.404	0.614
1	J1443	0.643	0.003	85.6	0.3	31.8	0.1	40.2820	0.2510	0.9895	0.0057	0.477	0.602
2	64° 5' 36.999" -132°	7.487	0.019	348.3	1.3	117.7	1.2	126.4998	1.3294	1.8232	0.0187	0.967	0.608
3	13'53.0004"	1.154	0.004	82.4	0.5	29.3	0.2	78.3031	0.5221	1.3591	0.0122	0.554	0.607
4		0.790	0.003	56.3	0.3	20.0	0.1	78.5263	0.4857	1.3630	0.0087	0.544	0.609
5		9.441	0.023	387.9	2.0	128.7	0.5	145.9664	0.6835	2.0024	0.0117	0.581	0.600
3	Well M	86.7780	0.2128	3150.7	15.6	1014.9	3.6	170.1028	0.7336	2.2867	0.0116	0.576	0.687
4		41.7632	0.1039	1378.0	6.9	435.6	1.5	190.7463	0.8186	2.4739	0.0123	0.575	0.680
5		243.8726	0.5974	4703.2	27.9	1254.8	4.4	386.6377	1.6394	4.3239	0.0213	0.574	0.687
6		25.6715	0.0637	781.9	4.3	242.3	0.9	210.7425	0.9610	2.6731	0.0147	0.584	0.691
7		133.9473	0.3272	2250.8	14.0	560.5	2.0	475.4030	2.0213	5.1705	0.0255	0.578	0.698
8		166.7851	0.4081	3403.1	20.0	931.4	3.3	356.2314	1.5233	4.0248	0.0202	0.572	0.674
1	J1719	0.738	0.002	50.6	0.3	17.9	0.1	81.8245	0.5768	1.3908	0.0095	0.684	0.605
2	64°50'47.8026" -	1.104	0.004	61.4	0.3	21.3	0.1	103.2652	0.6476	1.5954	0.0116	0.622	0.603
3	133°0'43.5564"	0.761	0.003	45.0	0.2	15.7	0.1	96.3474	0.7473	1.5345	0.0116	0.653	0.609
4		0.821	0.008	79.3	0.4	28.9	0.1	56.5053	0.8440	1.1432	0.0081	0.559	0.600
5		0.996	0.004	69.7	0.4	24.8	0.1	80.0356	0.5449	1.3700	0.0098	0.553	0.601
6		3.547	0.013	131.7	0.8	42.9	0.2	164.6136	1.0067	2.1850	0.0152	0.576	0.603
7		0.890	0.005	57.7	0.3	20.3	0.1	87.0138	0.9443	1.4346	0.0098	0.762	0.599
8		13.769	0.050	312.1	2.0	89.0	0.4	307.6607	1.7531	3.5544	0.0222	0.548	0.598

Uncertainties are given as  $2\sigma$  for  $^{187}\text{Re}/^{188}\text{Os}$  and  $^{187}\text{Os}/^{188}\text{Os}$  and  $^{192}\text{Os}$ .

The uncertainty includes the 2 SE uncertainty for mass spectrometer analysis plus uncertainties for Os blank abundance and isotopic composition.

<sup>a</sup> Rho is the associated error correlation (Ludwig, 1980).<sup>b</sup> Os<sub>i</sub> = initial  $^{187}\text{Os}/^{188}\text{Os}$  isotope ratio calculated at 578, 567, 575, 562 and 574 Ma.

Table S3: Geochronological data for Figure 3

Sample	Locality	Lithostratigraphy	Age (Ma) $\pm$ 2s analytical	$\pm$ 2s total	Age Type	Radiometric age details	Reference
17SWART7 ash 6 volcanic ash bed	Swartkloofberg section, Witputs Subbasin, Nama Basin, southern Namibia	Nomtsas Fm, Nama Group	538.58 $\pm$ 0.19	$\pm$ 0.63	$^{206}\text{Pb}/^{238}\text{U}$	Three of nine concordant single zircon grain analyses (excluding six older grains) combined to produce a weighted mean $^{206}\text{Pb}/^{238}\text{U}$ age, utilizing CA-TIMS and the EARTHTIME 535 spike.	Linnemann et al., 2019
BB5 volcanic ash bed	Oman (3045m depth, Birba-5 well)	Ara Group, 1m above base of A4 carbonate unit	541.00 $\pm$ 0.29	$\pm$ 0.63	$^{206}\text{Pb}/^{238}\text{U}$	Eight concordant single zircon grain analyses combined to produce a weighted mean $^{206}\text{Pb}/^{238}\text{U}$ age, utilizing CA-TIMS and the EARTHTIME 535 spike.	Bowring et al., 2007
sample 1.04 volcanic ash bed	Corcal, Corumbá - State of Mato Grosso do Sul, Brazil	top of Tamengo Formation, Corumba Group, southern Paraguay Belt	541.85 $\pm$ 0.77	$\pm$ 0.97	$^{206}\text{Pb}/^{238}\text{U}$	Five of eleven concordant single zircon grain analyses (excluding six older grains) combined to produce a weighted mean $^{206}\text{Pb}/^{238}\text{U}$ age, utilizing CA-TIMS and the EARTHTIME 535 spike.	Parry et al., 2017
sample 1.08 volcanic ash bed	Corcal, Corumbá - State of Mato Grosso do Sul, Brazil	top of Tamengo Formation, Corumba Group, southern Paraguay Belt	542.37 $\pm$ 0.32	$\pm$ 0.68	$^{206}\text{Pb}/^{238}\text{U}$	Four of eight concordant single zircon grain analyses (excluding 1 older and 3 younger grains) combined to produce a weighted mean $^{206}\text{Pb}/^{238}\text{U}$ age, utilizing CA-TIMS and the EARTHTIME 535 spike.	Parry et al., 2017
JIN04-2 volcanic ash bed	Jijawan (Jiuqunao) section, 17 km west of Maoping in Yangtze Gorges area, western Hubei Province, South China	top of Mishe member black shale, uppermost Doushantuo Fm	551.09 $\pm$ 0.84	$\pm$ 1.02	$^{206}\text{Pb}/^{238}\text{U}$	Sample JIN04-02 yields two concordant (of ten total) single zircon grain analyses with a weighted mean $^{206}\text{Pb}/^{238}\text{U}$ age of $551.09 \pm 1.02$ Ma. A corroborating weighted mean $^{207}\text{Pb}/^{206}\text{Pb}$ age of $548.09 \pm 2.61$ Ma is obtained from all ten zircons (recalculated using the U decay constant ratio of Mattinson, 2010).	Condon et al., 2005
Porto Morrinhos tuff	Porto Morrinhos - State of Mato Grosso do Sul, Brazil	Bocaina Formation, Corumba Group, southern Paraguay Belt	555.18 $\pm$ 0.34	$\pm$ 0.70	$^{206}\text{Pb}/^{238}\text{U}$	Nine concordant single zircon grain analyses combined to produce a weighted mean $^{206}\text{Pb}/^{238}\text{U}$ age, utilizing CA-TIMS and the EARTHTIME 535 spike.	Parry et al., 2017
volcanic ash bed, sample NoP-0.9	North Point, St. Mary's Bay, Avalon Peninsula, Newfoundland	post-glacial strata, basal Drock Formation, 0.9 m above the Gaskiers Formation; Conception Group	579.88 $\pm$ 0.52	$\pm$ 0.81	$^{206}\text{Pb}/^{238}\text{U}$	Five single zircon grains combined to produce a weighted mean $^{206}\text{Pb}/^{238}\text{U}$ age, utilizing CA-TIMS and the EARTHTIME 535 spike.	Pu et al., 2016
7S27 volcanic ash bed	Wangjilagou section in the Zhangcuping area, Yichang, Hubei Province, South China	between beds 3 and 4, below erosional unconformity in middle Doushantuo Fm	614.00 $\pm$ 9.00	$\pm$ 9.00	$^{206}\text{Pb}/^{238}\text{U}$	SHRIMP II ion probe analyses of 18 zircon grains yield a weighted mean $^{206}\text{Pb}/^{238}$ age of $614.0 \pm 9.0$ Ma (95% conf. int. including geologic scatter and an assumed 1% error in the TEMORA standardization).	Liu et al., 2009
SpB	Mackenzie Mountains, NW Canada	Sheepbed Formation, 0.9m above contact with Hayhook Limestone Formation	632.30 $\pm$ 3.4	$\pm$ 5.9	$^{187}\text{Re}-^{143}\text{Os}$	Re-Os isochron age from organic-rich carbonaceous mudstones. Regressed using Isoplot V.4.15 and includes the uncertainty in the $187\text{Re}$ decay constant from the Smolar et al. (1999) paper	Rooney et al., 2015
YG04-2 volcanic ash bed	Jijawan (Jiuqunao) section, 17 km west of Maoping in Yangtze Gorges area, western Hubei Province, South China	9.5m above base of Doushantuo Fm, 5m above top of Lower Dolomite Member (Nantuo Cap Carbonate)	632.48 $\pm$ 0.84	$\pm$ 1.02	$^{206}\text{Pb}/^{238}\text{U}$	Three concordant (of nine total) single zircon grain analyses have a weighted mean $^{206}\text{Pb}/^{238}\text{U}$ age of $632.48 \pm 1.02$ Ma. A corroborating weighted mean $^{207}\text{Pb}/^{206}\text{Pb}$ age of $629.97 \pm 2.83$ Ma is obtained from all nine zircons (recalculated using the U decay constant ratio of Mattinson, 2010).	Condon et al., 2005
YG04-15 volcanic ash bed	Wuhe-Gaojixi section, south of Sandouping in Yangtze Gorges area, western Hubei Province, South China	2.3m above base of Doushantuo Fm, within the Lower Dolomite Member (cap carbonate)	635.26 $\pm$ 0.84	$\pm$ 1.07	$^{206}\text{Pb}/^{238}\text{U}$	Three concordant (of 18 total) single zircon grain analyses have a weighted mean $^{206}\text{Pb}/^{238}\text{U}$ age of $635.26 \pm 1.07$ Ma. A corroborating weighted mean $^{207}\text{Pb}/^{206}\text{Pb}$ age of $632.97 \pm 2.82$ Ma is obtained from 11 zircons (recalculated using the U decay constant ratio of Mattinson, 2010).	Condon et al., 2005